A COMPARATIVE STUDY OF STRESS - FIELDS OF BLADE - DISC ATTACHMENT CONFIGURATIONS OF A TURBINE BLADE

by

PITAMBAR CHAUDHARY

DEPARTMENT OF MECHANICAL ENGINEERING

INDIAN INSTITUTE OF TECHNOLOGY, KANPUR

OCTOBER, 1990

A COMPARATIVE STUDY OF STRESS - FIELDS OF BLADE - DISC ATTACHMENT CONFIGURATIONS OF A TURBINE BLADE

A Thesis Submitted
in Partial Fulfilment of the Requirements
for the Degree of
MASTER OF TECHNOLOGY

by
PITAMBAR CHAUDHARY

to the
DEPARTMENT OF MECHANICAL ENGINEERING
INDIAN INSTITUTE OF TECHNOLOGY, KANPUR
OCTOBER, 1990

CERTIFICATE

This is to certify that the thesis entitled "**A Comparative Stu of Stress-Fields of Blade-Disc Attachment Configurations of Turbine Blade** ", by Pitambar Chaudhary is a record of work carri under our supervision and has not been submitted elsewhere for degree.

Dr N.S.Vyas
(Assistant Professor)
Dept. of Mechanical Engg.
I.I.T. Kanpur

Dr. P.M.Dixit
(Assistant Professor)
Dept. of Mechanical Engg.
I I.T. Kanpur

October, 1990

ACKNOWLEDGEMENT

I wish to express my deep sense of gratitude and indebtness to Dr. P.M. Dixit and Dr. N.S. Vyas for their inspiring guidance, invaluable suggestions and constructive criticism. They were always a constant source of encouragement throughout my thesis work.

I am thankful to Dr. N.N.Kishore for allowing me to use the P.C. facilities in ESA Lab.

I thank Mr. A.V. Rao, Mr. A.K. Keshari and Mr. K. Suresh Babu for their help rendered in completing my thesis. I feel happy to recall my association with all my friends during my stay at I.I.T. Kanpur.

— Pitambar Chaudhary.

CONTENTS

LIST OF FIGURES

LIST OF SYMBOLS

A	Area of cross-section
A', B'	Corner points
B	Width of the neck in tee-root
b_1, b_2	Width of the necks in straddle root
C	Thickness of the disc arm in tee-root
c_1, c_2	Thickness of the disc arms in the straddle root joint
C_1, C_2	Constants
E	Young's modulus of elasticity
F_z	Axial force
h	Axial thickness
L	Length of the shoulder in tee-root
l_1, l_2	Length of the shoulders in straddle root
l_b	Length of the blade
R_1	Outer radius of the disc
R_2	Inner radius of the disc
r, θ	Polar co-ordinates
T	Thickness of the shoulder in tee-root
t_1, t_2	Thickness of the shoulders in straddle root
u, w	Displacements X and Z directions
x, y, z	Cartesian co-ordinates
Z	Distance along the blade length
α	Angle made by tangential direction at the contact node with X-axis
$\varepsilon_r, \varepsilon_\theta$	Radial and circumferential strain
ρ	Density of the blade and disc material
ω	Angular velocity
μ	Co-efficient of friction
$\bar{\varepsilon}$	Clearance
$\varepsilon_x, \varepsilon_z$	Clearance in X and Z-directions in tee-root
$\varepsilon_{x1}, \varepsilon_{x2}$	Clearance in X-direction in straddle root
$\varepsilon_{z1}, \varepsilon_{z2}$	Clearance in Z-direction in straddle root
Γ	System boundary

Γ_q	Boundary on which forces are specified
σ_r, σ_θ	Radial and circumferential stress
σ_n, τ	Normal and shear stress
σ_g	Stress at the Gauss-integration point
σ_c	Stress at the nodal point
σ_{eq}	Equivalent stress at the corner point
$\bar{\sigma}_{eq}$	Non-dimensional equivalent stress in the optimum straddle root
$[(\sigma)_{opt}]_s$	Equivalent stress in the optimum straddle root
$(\sigma_{eq})_T$	Equivalent stress in the tee-root
$[B]$	Matrix containing the derivative of shape functions
$[D]$	Matrix containing material constants
$[K]$	Stiffness matrix
$[N]$	Matrix containing shape functions
$\{B_f\}$	Body force vector
$\{f\}$	Traction force vector
$\{F\}$	Force vector
$\{U\}$	Displacement vector
$\{\varepsilon\}$	Strain vector
$\{\sigma\}$	Stress vector

SUBSCRIPT AND SUPERSCRIPT	
A	Body A
B	Body B
e	Elemental
i,j,k	Dummy indices
n,s	Normal and tangential direction
T	Transpose

ABSTRACT

This work is a comparative study of stress-fields of the two most common blade-disc attachments of a turbine blade, namely tee and straddle. The study is restricted to only steady case i.e. it takes care of only the rotation of the disc but not the vibrations of the blade. For simplicity the blade is considered parallel to the disc and the placing of the root is assumed to be axial. The blade-disc attachment region is analysed as a plane stress contact problem by finite element method. The individual analysis of the blade and the disc provide the boundary conditions for the contact problem.

A finite element program is developed to find the equivalent stress at the corner points as well as stresses and displacements in the contact region. First the straddle root is optimised so that the equivalent stress at the corner points of both the shoulders become equal. Then the optimum straddle root is compared with tee-root of the same thickness to length (T/L) ratio for various values of this ratio. Finally normal and tangential stresses and displacements are presented for typical cases of tee and straddle roots.

CHAPTER I

INTRODUCTION

1.1 ROOT REGION OF A TURBINE BLADE :

The blades in a turbomachine are connected to the rotor by an attachment, called as "root region". The reliability of a turbomachine is affected by the reliability of its blades as well as the root region, as the failure of any of the blades or the root region leads to the failure of the turbine. Hence, a turbine blade and its root region must be strong enough to withstand different type of forces acting on it.

1.1.1 GEOMETRY OF THE ROOT REGION :

There are various ways of fixing turbine blades to the rotor. Any of the following methods can be used depending upon the application:

(1) Rotor and blades are machined as a single piece. Since this is an expensive arrangement, it is used in very special cases where the speed and working temperature of the rotor are very high.

(2) Blades are welded to the rotor. This arrangement is used in some gas turbines. Like the first type this arrangement also has light weight. But it is unsatisfactory from the maintenance point of view.

(3) Blades are inserted radially in a circumferential groove in the rotor. This arrangement is normally used in impulse turbine or in a low pressure stage of large turbines. In this case common shape of the roots are

dove-tail, tee or straddle.

(4) Blades are inserted axially in the axial slots spaced uniformly around the periphery of the rotor. This arrangement is normally used for fixing long blades in a low pressure stage of multistage turbine. The common shapes of the root for this case are fir-tree and, ball and shank type.

For the radial placing of the blade roots the circumferential groove is widened at one place. This is called the gate. The blades are inserted one at a time through the gate and slid around the slot until the circumference is nearly full. Finally the gate is closed by some special stop-piece. For balancing reason another similar gate is made at 180^{0} apart. Since the contact surface for the dove-tail root is inclined, the joint becomes loose when the turbine is subjected to repeated heating and cooling. On the other hand shoulder of tee and straddle roots give better grip to the blade. The straddle root is preferred when additional contact is required.

For axial placing of the blade roots the periphery is divided into as many points as the number of the blades in a single row. Sufficient axial spacing between the adjacent rotors is necessary to facilitate the insertion of the blades. In the case of large centrifugal force the axial dimension of the root should be wide enough to provide sufficient contact area.

1.1.2 STRESSES IN THE ROOT REGION

In the turbomachines the support provided by the disc to the blades is more like a rigid support. As a result maximum stresses occur in the root region of the blade. Further, because of the existance of the sharp corners, there is a stress concentration. Therefore, it is extremely important to carry out the stress analysis of the root region in general and critical corner points in the particular.

The stresses induced in the turbine blade are generally of two kinds. Those arising due to the rotation of the disc do not vary with time. These stresses have been termed as "steady stresses" in this thesis. The blades are also subjected to nozzle forces. These forces cause vibration of the blades and induce time dependent stresses in them. These can be called as "non-steady stresses". The complete dynamic analysis involves determination of both the steady as well as non-steady parts. The problem of the stress analysis of the root region, because of its complex geometry, is quite difficult even for the steady case. Addition of non-steady effect will make it even more difficult. Therfore, to keep the problem to the manageable level only steady-state stress analysis is considered.

While analysing the root region of a turbine blade its interaction with the surrounding slot of the disc has to be taken into account. This part of the disc does not behave any more rigidly than the root of

the blade. Thus the problem of the root region has to be treated as a problem of the stress analysis of two elastic bodies in contact. Such problems are called as "contact problems".

1.2 LITERATURE SURVEY ON THE CONTACT PROBLEM :

The first analytical approach to find the stresses and displacements in elastic bodies in contact with each other was proposed by Hertz [1]. This was a three dimensional problem based on certain assumptions. The two most important assumptions were that the area of contact was very small in comparison to the dimension of the bodies and the contact was frictionless. The three dimensional Hertz contact problem was simplified to an integral equation by I. Ya. Shtaerman [2]. Using this approach several contact problems were solved by Mushketishvili [3] and Gladwell [4]. However, all the contact problems solved so far have simple geometries. No wonder, the problem of the root region of a turbine blade does not figure in this list.

1.2.1 REFERENCES USING FINITE ELEMENT METHOD :

There have been many attempts to use numerical methods to solve contact problems. The most widely used method is the finite element method (FEM). One of the earliest important reference as on use of FEM in solution of the contact problem is that of Francavilla and Zienkiewicz [5]. They solved the frictionless contact problem by treating it as quasi-linear problem. N. Okamoto and M. Nakazawa [6] proposed a finite element method based

on load incremental theory taking friction into account. Hung and Sauxe [7] used FEM and mathematical programming techniques to solve frictionless contact problems. The problem was solved as a non-iterative optimisation problem where the contact conditions were linearised in a suitable fashion. Sachdeva and Ramakrishnan extended the method of Francavilla and Zienkiewicz to take care of force boundary conditions [8] and frictional effects under proportionate loading [9]. Torstenfelt [10] proposed a general purpose finite element computer program to solve contact problems with friction. Rahman et. al. [11] used finite element incremental procedure for contact analysis where one of the bodies is rigid. The contact condition at a node is established when it penetrates or touches the rigid body. Bathe and Chaudhary [12] presented a procedure for the analysis of plannar and axisymmetric contact problems involving sticking, frictional sliding and separation under large deformation. Contact of a cylinder with a rigid plane, motion of a rubber sheet in a converging channel and analysis of a buried pipe were solved as illustrative problems. Chandrasekhra et. al. [13] solved the contact problem by imposing geometric constraints on the pseudo equilibrium configuration defined as a configuration at which the compatibility conditions are violated.

The first reference on use of FEM in analysis of a turbine blade root region is that of Cham and Tuba [14]. They have used triangular elements to study the fir-tree root. Their results show that the coefficient of friction

has only a marginal effect on stresses and displacements in the root region but the effect of the clearance between blade root shoulder and disc arm is quite significant. However, the detailed results are not presented. Srivastava [15] analysed the tee-root to study the effects of rotor speed and the clearance around the root shoulder on the contact stresses and displacements. The four noded isoparametric elements were used.

1.3 OBJECTIVE AND SCOPE OF THE PRESENT WORK :

The present work is an attempt to carry out the steady-state stress analysis of the blade-disc attachment configuration of a turbine blade. The study is restricted to only two configurations namely tee-shaped and straddle roots. The objective is to compare these configurations from the point of equivalent stress at the corner points. The configurations are shown in Figs.1.1 and 1.2. The straddle has two necks. We have considered two different models of straddle root. In the first model the width of both the necks are equal while in the second the width of the lower neck is reduced appropriately. This has been done keeping in mind the fact that the lower neck is subjected to less axial load compared to the top neck. The straddle root also has two shoulders and hence two critical points. The equivalent stresses at these two corner points depend on relative lengths and thicknesses of the shoulders. In the optimum design of a straddle root, equivalent stress at both the corner points should be equal so as to make effective use of

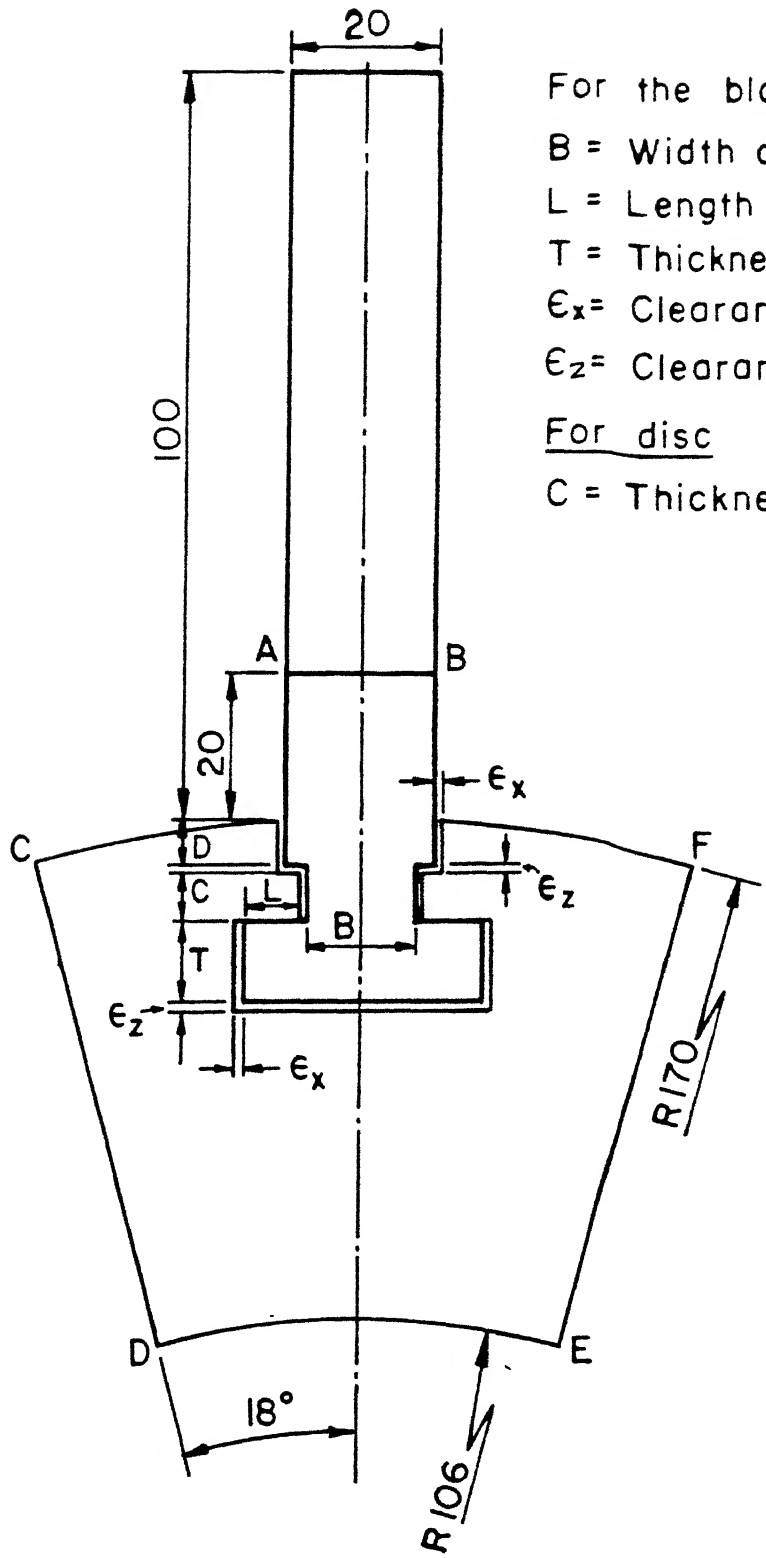

For the blade

B = Width of the neck

L = Length of the shoulder

T = Thickness of the should

ϵ_x = Clearance in x direction

ϵ_z = Clearance in z direction

For disc

C = Thickness of disc arm

AB and CDEF boundaries define the root domain.

Inner radius of disc = 50 mm.

Fig. 1.1 The Tee root joint between the blade and disc

AB and CDEF boundaries define the blade and disc straddle

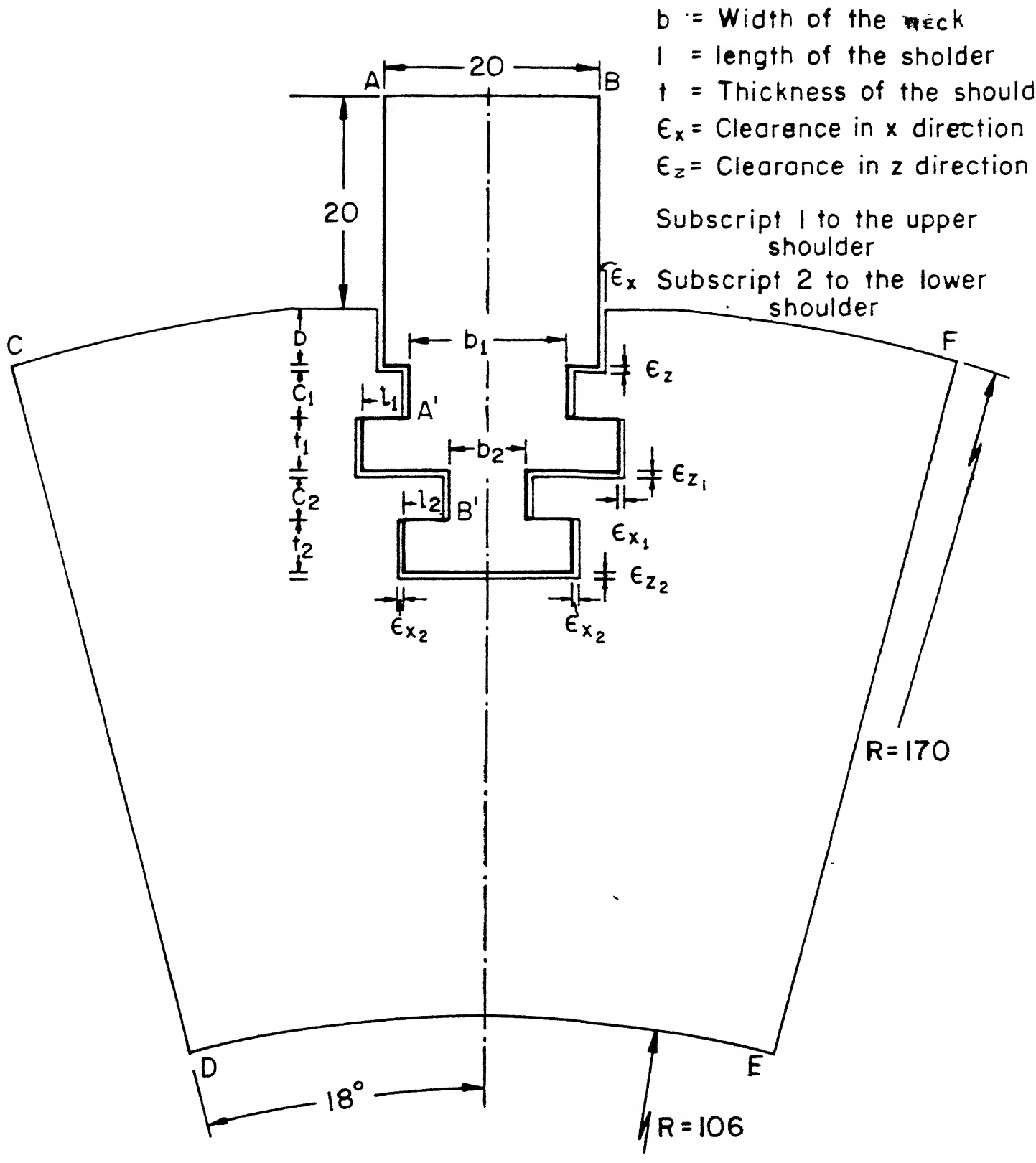

Fig 1.2 Straddle root joint between the blade and disc

both the shoulders. The optimum case is obtained by varying the ratio of lengths of the shoulders. The straddle root with the optimum ratio of shoulders length is henceforth referred as "optimum straddle". This optimum straddle root is compared with a tee-root. Since there has to be some common ground for comparison, the total contact area in both the roots is kept the same. This means the sum of the lengths of the two shoulders of the straddle root is made equal to the length of the tee-root. The thicknesses of the two shoulders of the straddle root are taken in proportion to their lengths and their sum is made equal to the thickness of the shoulder of the tee-root. Similar policy is adopted about various clearances. Thus the relations between various geometric parameters of straddle and tee root are given by

$$
\left.
\begin{aligned}
& l_1 + l_2 = L \\
& t_1 + t_2 = T \\
& \text{where} \quad \frac{t_1}{l_1} = \frac{t_2}{l_2} \\
& \omega_{x_1} + \omega_{x_2} = \omega_x \\
& \text{where} \quad \frac{\omega_{x_1}}{l_1} = \frac{\omega_{x_2}}{l_2} \\
& \omega_{z_1} + \omega_{z_2} = \omega_z \\
& \text{where} \quad \frac{\omega_{z_1}}{l_1} = \frac{\omega_{z_2}}{l_2}
\end{aligned}
\right\} \qquad (1.1)
$$

(see the Figs. 1.1(a) and 1.1(b)). The comparison of the tee and straddle roots is made for various values of the thickness to length (T/L) ratio.

The blade is normally staggered with respect to the disc. This makes the actual problem three-dimensional. However to keep things simple, we assume the blade to be in the plane of the disc. Further it is assumed that the blade is inserted axially. Because of these two assumptions, the problem can now be considered as a plane stress problem. Finally the blade is idealised as a bar of uniform rectangular cross-section and the disc thickness is assumed to be uniform. First the blade is analysed as a bar subjected to variable body force resulting from the rotation of the disc and the disc is analysed as a body in the state of axisymmetric plane state and subjected to variable body force in the radial direction. But this analysis becomes invalid in the root region because of the change in geometry and interaction between the blade and disc. To analyse the root region, a domain consisting of appropriate portions of the blade and disc surrounding the actual contact area is chosen as shown in Fig. 1.2 . The boundaries of the domain adjoining the blade and the disc (i.e. the boundaries AB, CD, DE and EF) have to be at a sufficiently large distance from the contact area so that the analysis of the blade and the disc, as done above, remain valid upto these boundaries. In fact, the stress boundary conditions on these boundaries are provided by the blade and the disc analysis. The root region is

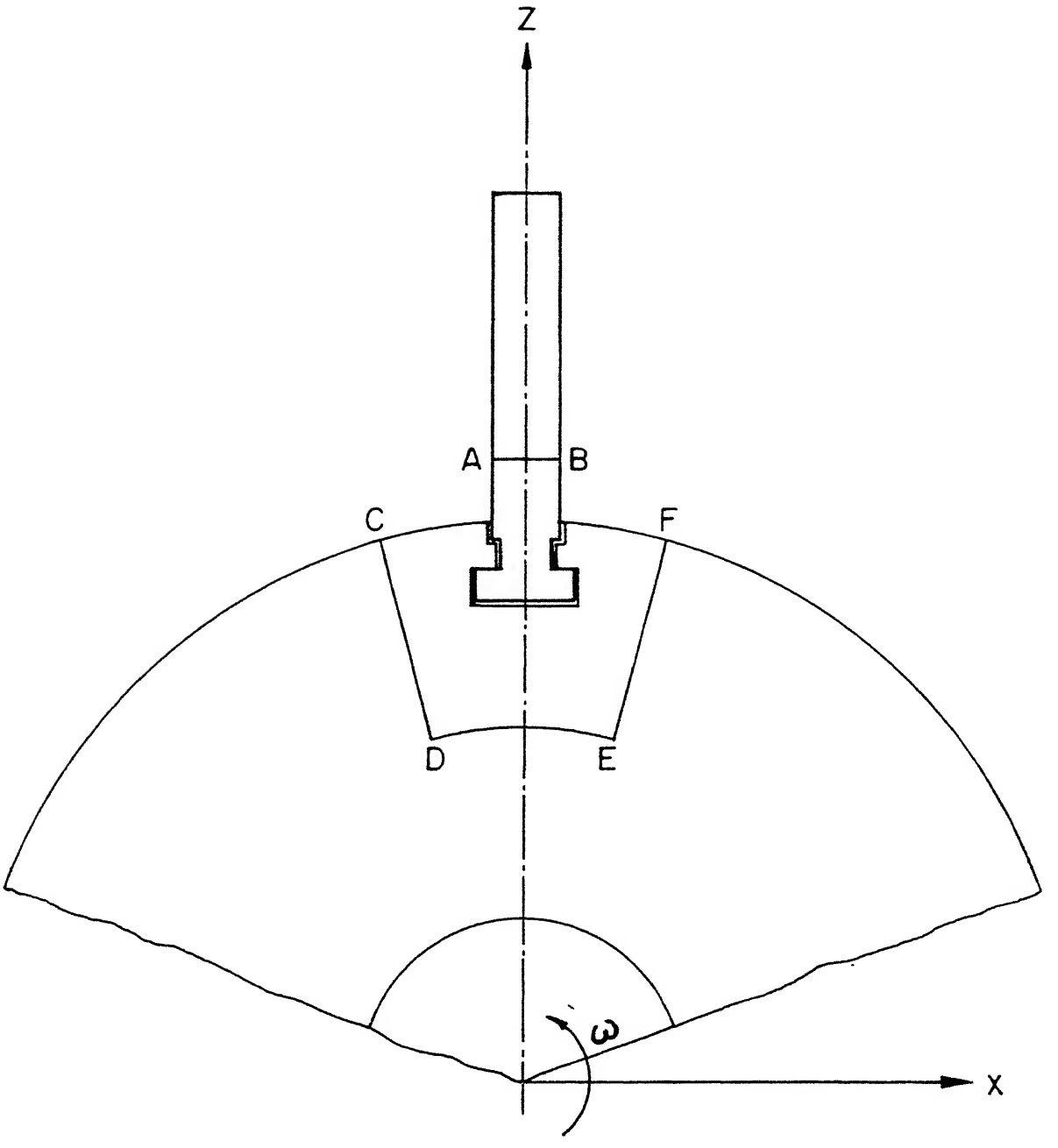

Fig. 1.3 Root domain for the contact problem.
(Tee-root)

analysed as a plane stress contact problem using Finite Element Method.

A computer program is developed to determine the equivalent stress at the corner points of the shoulder as well as to evaluate the stresses and displacements in the contact region. First the tee-root is analysed to obtain the variation of the equivalent stress at the corner point with respect to thickness to length (T/L) ratio. Then for a given T/L ratio, the models of straddle root are analysed to find the optimum ratio of shoulder lengths (l_1/l_2). At the optimum value, the equivalent stresses at both the corners becomes equal. Finally the equivalent stress in the optimum straddle root is compared with the equivalent stress in the tee-root with the same T/L ratio. This is done to obtain the range of T/L ratio for which the straddle root is better than the tee-root i.e. has a lesser value of the equivalent stress. Variation of the contact stresses and displacements for both the tee and straddle roots is reported for the lowest T/L ratio from the favourable range.

This study has several limitations in the form of approximations and idealisations made as under.

(1) The study is restricted to only steady conditions. Under unsteady conditions the range of T/L ratios for which the straddle root becomes better than the tee-root may change.

(2) The blades with tee or straddle roots are usually fixed radially. But this type of attachment makes the

problem three-dimensional. To reduce the problem to a state of plane stress the blades are assumed to be fixed axially.

(3) The blade is analysed as a rectangular bar of uniform cross-section under axial loading. But the actual blade is tapered, twisted, and has an aerofoil cross-section.

(4) The disc is considered as an axisymmetric body of uniform thickness. However, in practice, the disc with axial slots is not axisymmetric. Moreover, the thickness of the disc varies in the radial direction.

1.4 PLAN OF THE THESIS :

The formulation of the blade, disc and contact problem are discussed in Chapter II. The solution procedure for the contact problem is also described here. The Chapter III contains the results and discussions. The conclusions and suggestions for future work are given in Chapter IV.

CHAPTER II

THE FORMULATION

2.1 THE BLADE :

The blade is treated as a bar of uniform rectangular cross-section mounted on a rotating disc, (Fig. 2.1). The axial stress induced in the blade due to disc rotation is evaluated as follow.

The centrifugal force on a small element of length dZ at a distance Z from the root of the blade (Fig. 2.1) is given by

$$dF = \rho\, \omega^2\, A\, (R_1 + Z)\, dZ$$

Therefore the axial force on a section at the distance Z is given by

$$F = \int_{Z}^{l_b} \rho\, \omega^2\, A\, (R_1 + Z)\, dZ$$

$$= \rho\, \omega^2\, A \left[R_1 Z + \frac{Z^2}{2} \right]_{Z=Z}^{Z=l_b}$$

Now the axial stress σ_z on this sector is given by

$$\sigma_z = \frac{F}{A}$$

$$= \rho\, \omega^2 \left[R_1\, (l_b - Z) + \frac{(l_b^2 - Z^2)}{2} \right] \qquad (2.1)$$

2.2 THE DISC :

The disc is assumed to be of uniform thickness clamped at its inner boundary on a shaft which is rotating at a constant angular velocity ω about the Y-axis (Fig. 2.1). The disc is in a state of axisymmetric as well as plane stress. There is only one nontrivial equation of motion. In

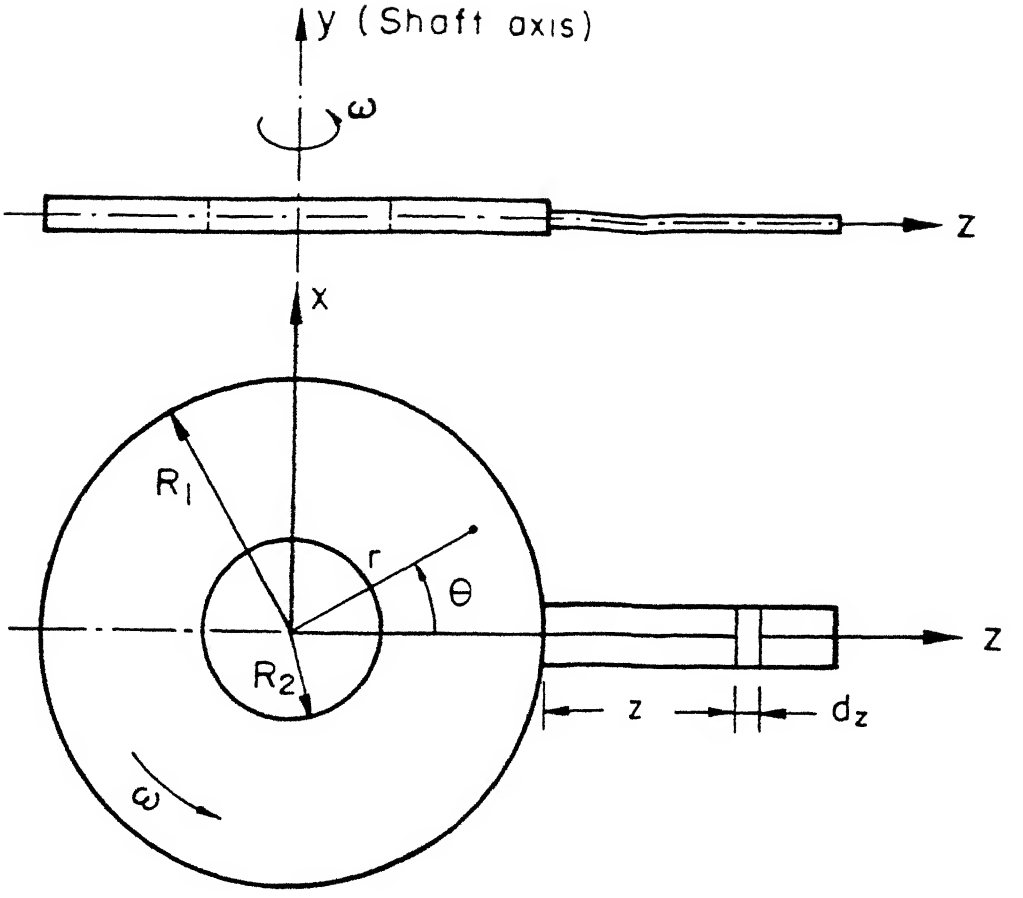

Fig. 2.1 Blade mounted as a rotating disc.

terms of stress components, it is given by

$$\frac{d\sigma_r}{dr} + \frac{\sigma_r - \sigma_\theta}{r} + \rho\omega^2 r = 0 \qquad (2.2)$$

Since it is one equation in two unknowns, it cannot be solved in the present state. However, it can be solved by expressing it in terms of the radial displacements.

For the axisymmetric plane stress problem, the stress-strain relations are

$$\sigma_r = \frac{E}{1-\nu^2}\left(\varepsilon_r + \nu\,\varepsilon_\theta\right)$$

$$\sigma_\theta = \frac{E}{1-\nu^2}\left(\varepsilon_\theta + \nu\,\varepsilon_r\right) \qquad (2.3)$$

and the strain displacement relations are

$$\varepsilon_r = \frac{du_r}{dr} \quad ; \quad \varepsilon_\theta = \frac{u_r}{r} \qquad (2.4)$$

Substituting the relations (2.3) and (2.4) into (2.2) we get

$$\frac{E}{1-\nu^2}\frac{d}{dr}\left[\frac{1}{r}\frac{d}{dr}(r\,u)\right] + \rho\omega^2 r = 0 \qquad (2.5)$$

the solution of this equation is

$$u_r = -\frac{1-\nu^2}{E}\rho\omega^2\frac{r^3}{8} + C_1 r + \frac{C_2}{r} \qquad (2.6)$$

where C_1 and C_2 are constants of integration.

Substituting the expression (2.6) for the radial displacement into the equation (2.4) and (2.3) we get the following expression for stresses

$$\sigma_r = C_1\frac{E}{1-\nu} - \frac{C_2}{r^2}\frac{E}{1+\nu} - \frac{3+\nu}{8}\rho\omega^2 r^2 \qquad (2.7)$$

$$\sigma_\theta = C_1\frac{E}{1-\nu} + \frac{C_2}{r^2}\frac{E}{1+\nu} - \frac{1+3\nu}{8}\rho\omega^2 r^2 \qquad (2.8)$$

The constants C_1 and C_2 are to be determined from the boundary conditions. Since the shaft to which the disc is attached is relatively more rigid than the disc, at the boundary $r = R_2$ the boundary condition becomes

$$u_r = 0 \quad \text{at} \quad r = R_2 \ . \tag{2.9}$$

The boundary $r = R_1$ is stress free. Therefore

$$\sigma_r = 0 \quad \text{at} \quad r = R_1 \tag{2.10}$$

Using these conditions, we get

$$C_1 = \frac{1-\nu}{1+\nu} \frac{C_2}{R_1^2} + \frac{(3+\nu)(1-\nu)}{8\,E} \rho\, \omega^2\, R_1^2 \tag{2.11}$$

with

$$C_2 = - \frac{(1-\nu^2)\rho\, \omega^2\, R_1^2\, R_2^2}{8E} \left[\frac{(3+\nu)R_1^2 - (1+\nu)R_2^2}{(1+\nu)R_1^2 + (1-\nu)R_2^2} \right] \tag{2.12}$$

2.3 FEM FORMULATION OF THE CONTACT PROBLEM :

As stated earlier the root region of the turbine blade is analysed as a contact problem. The domain of the problem is shown in Fig. 1.2. The boundary conditions for the problem come from the analysis of section 2.1 and 2.2. Since the domain is a plate like region and stresses on the boundaries are constant across the thickness, this contact problem can be treated as a plane stress problem.

2.3.1 FEM SOLUTION PROCEDURE :

In FEM formulation, the governing equations (partial differential equations) are converted into an equivalent set of algebraic equations. There are two common procedures available for converting the governing equations into

equivalent algebraic equations. These are (i) the variational procedure and (ii) the Galerkin procedure (or the method of weighted residues). The solution domain is divided into several small elements of chosen shape and the unknown field variables are expressed in terms of assumed approximating functions (or interpolation functions) within each element. The approximating functions are defined within each element in terms of the field variables at specified points called as nodes The nodal values of the field variables and the interpolation functions for the element completely define the behavior of the field variables within the element. For the finite element formulation of the problem, the nodal values of the field variables become the unknowns. The algebraic equations of the element involve integration of the interpolation functions or their derivatives over the element. All such elemental integrals are assembled to obtain the final matrix equation. The unknown nodal variables are calculated by solving the assembled matrix equation for the whole solution domain.

2.3.2 FEM FORMULATION FOR PLANE STRESS :

Consider a body Ω of uniform thickness h bounded by two parallel planes $Y = -h/2$ and $Y = h/2$ and a closed boundary Γ (Fig. 2.2). The part of the boundary on which external stresses act is denoted by q . The body is in a state of plane stress. Although σ_y is not zero, it is not required in the analysis. Only the strain

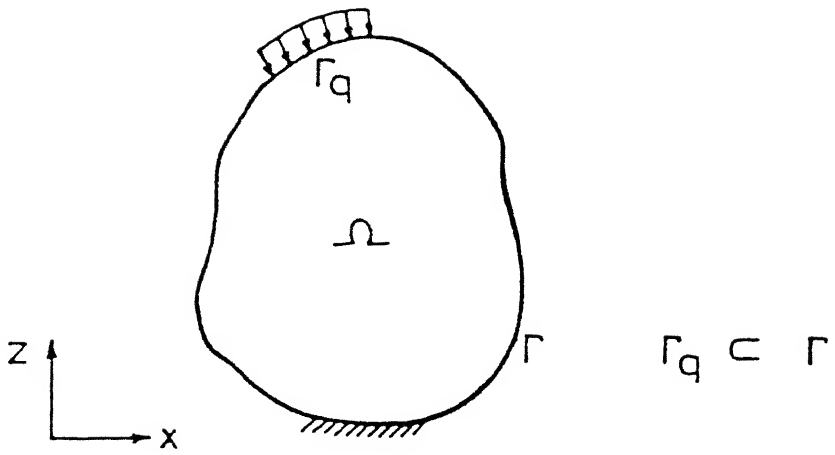

Fig. 2.2 Body in plane stress

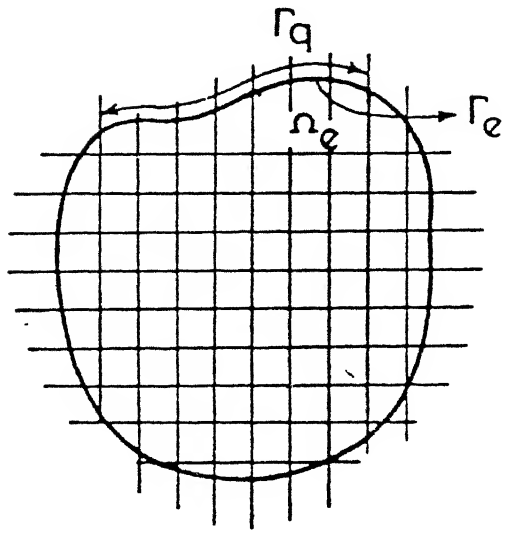

Fig. 2.3 Discretisation of the domain.

components in X-Z plane are needed. The strain-displacements relation in this plane are

$$\varepsilon_x = \frac{\partial u}{\partial x} \quad ; \quad \varepsilon_z = \frac{\partial w}{\partial z} \quad ; \quad \gamma_{xz} = \frac{\partial u}{\partial z} + \frac{\partial w}{\partial x}$$

In matrix form

$$\{ \varepsilon \} = [L] \{ u \} \tag{2.13}$$

Where $\{ \varepsilon \} = \{ \varepsilon_x \quad \varepsilon_z \quad \gamma_{xz} \}^T$

$\{ u \} = \{ u \quad w \}^T$

$$[L] = \begin{bmatrix} \frac{\partial}{\partial x} & 0 \\ 0 & \frac{\partial}{\partial z} \\ \frac{\partial}{\partial z} & \frac{\partial}{\partial x} \end{bmatrix} \tag{2.14}$$

Then stress strain relationship for a homogeneous, isotropic, linearly elastic material under plane stress conditions is given by

$$\{ \sigma \} = [D] \{ \varepsilon \} \tag{2.15}$$

Where $\{ \sigma \} = \{ \sigma_x \quad \sigma_z \quad \tau_{xz} \}^T$

and $$[D] = \frac{E}{1-\nu^2} \begin{bmatrix} 1 & \nu & 0 \\ \nu & 1 & 0 \\ 0 & 0 & \frac{\nu-1}{2} \end{bmatrix} \tag{2.16}$$

The strain energy is

$$U = \int_A \frac{1}{2} \{ \varepsilon \}^T \{ \sigma \} \, h \, dA \tag{2.17}$$

If

$$\left\{ f \right\} = \begin{Bmatrix} f_x \\ f_z \end{Bmatrix} \quad \text{and} \quad \left\{ B_f \right\} = \begin{Bmatrix} B_x \\ B_z \end{Bmatrix} \tag{2.18}$$

represent the applied traction on Γ_q and the body force

(per unit volume) respectively, then the work done by the external forces is given as

$$W_p = \int_A \{ u \}^T \{ B_f \} h \, dA + \int_{\Gamma_q} \{ u \}^T \{ f \} h \, dl \qquad (2.19)$$

The expression for Potential Energy of the system is given as

$$\Pi_p = U - W_p \qquad (2.20)$$

Using Eqs. (2.15), (2.17), and (2.19)

$$\Pi_p = \frac{1}{2}\int_A \{ \varepsilon \}^T [D] \{ \varepsilon \} h dA - \int_A \{ u \}^T \{ B_f \} h dA - \int_{\Gamma_q} \{ u \}^T \{ f \} h dl \qquad (2.21)$$

Let the domain be divided into N_e number of elements (Fig.2.3). Over a typical element e, let

$$\{ u \} = \begin{bmatrix} N_1 & 0 & \ldots & N_n & 0 \\ 0 & N_1 & \ldots & 0 & N_n \end{bmatrix} \begin{Bmatrix} u_1^e \\ w_1^e \\ \vdots \\ u_n^e \\ w_n^e \end{Bmatrix}$$

$$= [N] \{ u \}_{nodal} \qquad (2.22)$$

be the approximation for the displacement vector, where n is the number of nodes per element u_1^e, w_1^e, ...u_n^e, w_n^e are the displacements at the nodes and $N_1 \ldots N_n$ are the shape functions in the form of polynomials of the coordinates x and z. Then from equation (2.13), we get

$$\{ \varepsilon \} = [B] \{ u \}_{nodal} \qquad (2.23)$$

Where the matrix [B] contains the derivatives of the shape functions. Substituting Equations (2.22) and (2.23) in

to the expression (2.21) for the potential energy, we get

$$\Pi_p = \sum_{e=1}^{N_e} \frac{1}{2} h \int_{A_e} \{ u \}^T_{nodal} [B]^T [D] [B] \{ u \}_{nodal} \, dA$$

$$- \sum_{e=1}^{N_e} h \int_{A_e} \{ u \}^T_{nodal} [N]^T \{ B_f \} dA - \sum_{e=1}^{N_b} h \int_{\Gamma_e} \{ u \}^T_{nodal} [N]^T \{ f \} dl \qquad (2.24)$$

Here Γ_e is the boundary of an element which is common with Γ_q and N_b is the number of such elements (Fig. 2.3).

Setting the first variation of Π_p to zero, we get

$$[K] \{ U \} = \{ F \} \qquad (2.25)$$

Where

$$[K] = \sum_{e=1}^{N_e} [K]^e \qquad (2.26)$$

$$[K]^e = \int_{A_e} [B]^T [D] [B] h \, dA \qquad (2.27)$$

$$\{ F \} = \sum_{e=1}^{N_e} \{ F \}^e \qquad (2.28)$$

$$\{ F \}^e = \int_{A_e} [N]^T \{ B_f \} h \, dA + \int_{\Gamma_e} [N]^T \{ f \} h \, dl \qquad (2.29)$$

and $\{ U \}$ is the vector of nodal displacements for the entire domain.

In the equation (2.26) and (2.28), it is understood that the sum is performed after expanding $[\ K\ ]^e$ and $\{\ f\ \}^e$ to the full size.

2.3.3 FORMULATION OF THE CONTACT PROBLEM :

Two bodies A and B which are in the state of plane stress are in contact with each other as shown in Fig 2.4. The finite element equations for these bodies are

$$\left[K_A \right] \left\{ U_A \right\} = \left\{ F_A \right\} \qquad (2.30a)$$

$$\left[K_B \right] \left\{ U_B \right\} = \left\{ F_B \right\} \qquad (2.30b)$$

where $\left[K_A \right]$, $\left[K_B \right]$, $\left\{ U_A \right\}$, $\left\{ U_B \right\}$, $\left\{ F_A \right\}$, $\left\{ F_B \right\}$ are the stiffness matrices, displacement vectors and force vectors of bodies A and B respectively. The force vector includes the contact forces also.

The equations (2.30) cannot be solved as at the contact nodes, neither displacements nor forces are known. To overcome this difficulty, contact conditions are used.

Before applying the contact conditions, it is convenient to combine the equations (2.30a) and (2.30b) into one single equation.

$$\begin{bmatrix} [K_A] & 0 \\ 0 & [K_B] \end{bmatrix} \begin{Bmatrix} \{U_A\} \\ \{U_B\} \end{Bmatrix} = \begin{Bmatrix} \{F_A\} \\ \{F_B\} \end{Bmatrix}$$

or $$[\ K\ ]\{\ U\ \} = \{\ F\ \} \qquad (2.31)$$

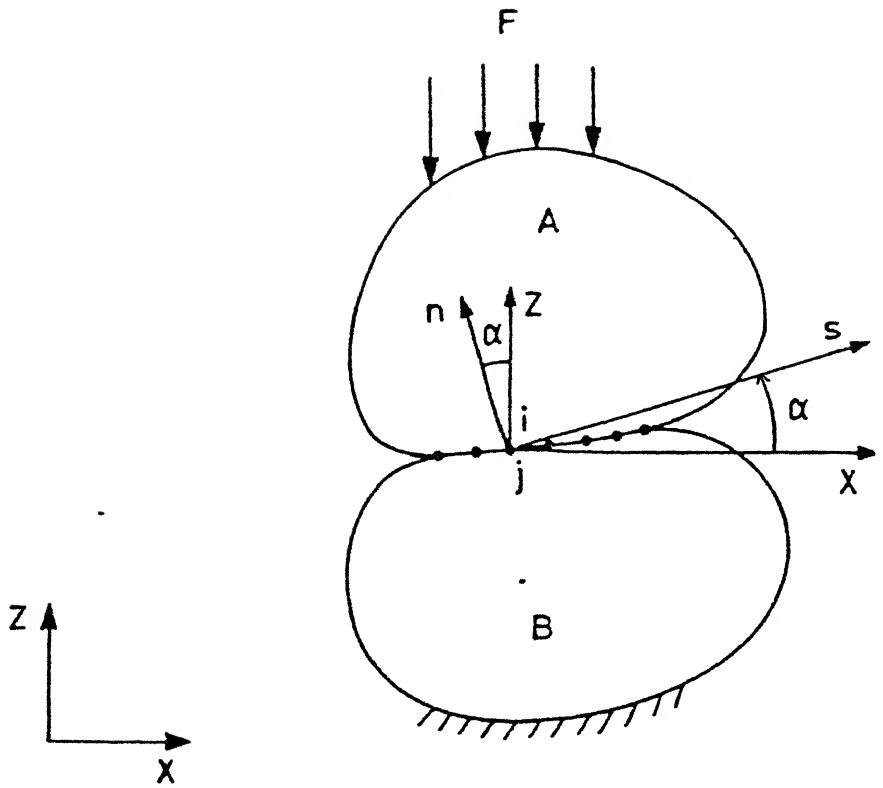

Fig. 2.4 Two bodies A and B in contact.

2.3.3.1 CONTACT CONDITIONS :

There are two sets of contact conditions, one on the unknown contact forces and the other on the displacements. Let i^{th} node of body A be in contact with the j^{th} node of body B (Fig. 2.4). Let n and s denote respectively the normal and the tangential directions at the contact node. Then the conditions on forces, as given by Newton's third law, are

$$\left[F_A \right]_{in} = - \left[F_B \right]_{jn} \tag{2.32}$$

$$\left[F_A \right]_{is} = - \left[F_B \right]_{js} \tag{2.33}$$

The compatibility of displacement components gives the second set of condition

$$- \left\{ U_A \right\}_{in} + \left\{ U_B \right\}_{jn} = \bar{\delta} \tag{2.34}$$

$$\left\{ U_A \right\}_{is} = \left\{ U_B \right\}_{js} \tag{2.35}$$

where $\bar{\delta}$ denotes the clearance

The compatibility condition for the tangential direction is valid only when there is no slip between the contact nodes. The slip depends on the magnitude of the normal force at the node and the coefficient of friction between the bodies in contact. In the case of slip, the condition (Eq. 2.35) on tangential displacement should be replaced by the following relation

$$\left| \left(F_B \right)_{js} \right| = \mu \left| \left(F_B \right)_{jn} \right| \qquad (2.36)$$

This condition can be applied to the body A also.

The contact conditions (2.32)-(2.36) are in terms of the components with respect to normal and tangential directions, while the finite elements equation (2.31) are with respect to X-Z coordinate system. Therefore, first, these conditions must be expressed in terms of the X-Z components. From the Fig.2.4, we get the following relations between the n-s components and X-Z components.

$$(F_A)_{in} = -(F_A)_{ix} \text{ Sin } \alpha + (F_A)_{iz} \text{ Cos } \alpha \qquad (2.37)$$

$$(F_A)_{is} = (F_A)_{ix} \text{ Cos } \alpha + (F_A)_{iz} \text{ Sin } \alpha \qquad (2.38)$$

Here α is the angle which s-directions makes with x-axis. Similarly, the normal and tangential components of other forces and displacements can be expressed in terms of the X-Z components. Substituting the Eq. (2.37)-(2.38) and similar relation for $(F_B)_{jn}$, $(F_B)_{js}$, $(U_A)_{in}$, $(U_A)_{is}$, $(U_B)_{jn}$ and $(U_B)_{js}$ into the Eq.(2.32)-(2.36), we get the following conditions

$$-(F_A)_{ix} \text{ Sin } \alpha + (F_A)_{iz} \text{ Cos } \alpha - (F_B)_{jx} \text{ Sin } \alpha + (F_B)_{jz} \text{ Cos } \alpha = 0 \qquad (2.39)$$

$$(F_A)_{ix} \text{ Cos } \alpha + (F_A)_{iz} \text{ Sin } \alpha + (F_B)_{jx} \text{ Cos } \alpha + (F_B)_{jz} \text{ Sin } \alpha = 0 \qquad (2.40)$$

$$(U_A)_{ix} \text{ Sin } \alpha - (U_A)_{iz} \text{ Cos } \alpha - (U_B)_{jx} \text{ Sin } \alpha + (U_B)_{jz} \text{ Cos } \alpha = \bar{\delta} \qquad (2.41)$$

$$(U_A)_{ix} \text{ Cos } \alpha + (U_A)_{iz} \text{ Sin } \alpha - (U_B)_{jx} \text{ Cos } \alpha - (U_B)_{jz} \text{ Sin } \alpha = 0 \qquad (2.42)$$

$$(ss\ \cos\alpha + \mu\ sn\ \sin\alpha\ )(F_B)_{jx} + (ss\ \sin\alpha - \mu\ sn\ \cos\alpha)(F_B)_{jz} = 0 \qquad (2.43)$$

where ss is sign of $(F_B)_{js}$ and sn is sign of $(F_B)_{jn}$ Note that in case of no slip the condition (2.42) applies while the condition (2.43) is to be used when there is slip.

2.3.3.2 APPLICATION OF CONTACT CONDITIONS :

It can be seen that corresponding to every contact pair (i,j), there are four equations in the set (2.31) : two equations - (2i-1)th Eq. for x-direction and (2i)th Eq. for z-direction, for the body A and the remaining two (2j-1)th Eq. and (2j)th, for the body B. At stated earlier, neither the displacement associated with these nodes nor the forces (i.e. the right hand side of these equations) are known. Therefore, these equations can not be solved as such. However for every contact pair, there are four contact conditions. Our strategy is to replace these equations with unknown right hand sides by the contact conditions which have the known right hand side. The matrix operations required for this process are described below.

First we replace the (2i-1)th Eq. of body A by the Eq.(2.39). Since $(F_A)_{ix}$ and $(F_A)_{iz}$ are equal to the left hand sides of (2i-1)th and (2i)th Eq. of the body A and $(F_B)_{jx}$ and $(F_B)_{jz}$ are equal to the left hand side of (2j-1)th and (2j)th Eq. of body B, the condition states that

(−sinα) (2i−1)th Eq. of body A

+(cosα) (2i)th Eq. of body A

+(−sinα) (2j−1)th Eq. of body B

+(cosα) (2j)th Eq. of body B =0

Thus after replacement, the (2i−1)th row of the $[K_A]$ becomes equal to

(−sinα)(2i−1)th row of $[K_A]$

+(cosα)(2i) th row of $[K_A]$

+(−sinα)(2j −1) th row of $[K_B]$

+(cosα)(2j) th row of $[K_B]$

The (2i−1)th row of $[F_A]$, of course, becomes zero.

Next, the (2i)th Eq. of body A is replaced by the Eq. (2.40). The matrix operations for this replacement are similar. Now, the (2i) th row of $[K_A]$ is replaced by the linear combination of (2i−1)th and (2i)th rows of $[K_A]$ and (2j−1)th and (2j) th rows of $[K_B]$, the coefficients of a linear combination given by the Eq. (2.40). The (2i)th row of $[F_A]$, of course, becomes zero. Note that the Eq.(2.40) involves the original (2i−1)th row of $[K_A]$ and not the modified one. Thus (2i−1)th row of $[K_A]$ has to be stored before applying the first contact condition.

The third condition is applied in the end. The reasons for this change of order will be explained later. So now, consider the fourth contact condition. We use this to replace (2j−1)th Eq. of body B. In case of no slip the condition is given by the Eq. (2.42). Since this Eq. is

in terms of displacement components, we don't have to do any row operation like the first two conditions while using it for replacement. Instead, we simply have to replace the (2j-1)th row of $[K_B]$ by zeros except in the columns (2i-1), (2i), (2j-1) and (2j). In these columns, the new coefficients will be respectively $\cos\alpha$, $\sin\alpha$, $(-\cos\alpha)$ and $(-\sin\alpha)$. The (2j-1)th row of $[F_B]$, of course, becomes zero. In case of slip, the condition is given by the Eq. (2.43). This condition is similar to the first two conditions except that it involves only two Eq. : (2j-1)th and (2j) th equations of body B. So here, (2j-1)th row of $[K_B]$ is replaced by the linear combinations of (2j-1)th and (2j) th rows of $[K_B]$, the coefficients of the linear combination given by Eq. (2.43). The (2j-1)th row of $[F_B]$ is, of course, made zero. Finally, the (2j) th Eq. of body B is replaced by the third contact condition (Eq. 2.41). Since it is in terms of the displacement components, we simply have to replace the (2j)th row of $[K_B]$ by zeros. except in the columns (2i-1), (2i), (2j-1) and (2j) where the new coefficients will be $\sin\alpha$, $(-\cos\alpha)$, $(-\sin\alpha)$ and $\cos\alpha$. The (2j)th row of $[F_B]$ is made equal to $\bar{\epsilon}$ (the clearance).

If we apply the third Eq. before the fourth, then the (2j)th Eq. of body B gets modified. In case of slip, the original (2j)th Eq. is needed to apply the fourth condition. So either we store the (2j)th row of $[K_B]$ and then apply the third and fourth condition in that order or we reverse the order and don't store the (2j)th row of

$[K_B]$. The later alternative is more convenient and followed here.

2.3.3.3 SUB-STRUCTURING :

Since the number of contact nodes is initially unknown, an iterative procedure needs to be applied to the Eq.(2.31). Further imposition of the contact conditions renders the stiffness matrix unsymmetric. An iterative scheme involving large unsymmetric matrices requires a large storage and a considerable amount of computing time. To reduce both storage and computational time, the stiffness matrix is stored in skyline form and then decomposed to a much smaller size using substructuring.

First step in substructuring is to rearrange the rows and columns of the global stiffness matrix as shown below

$$\begin{bmatrix} K_{I,I} & K_{I.II} & K_{I,III} \\ K_{II,I} & K_{II,II} & K_{II,III} \\ K_{III,I} & K_{III,II} & K_{III,III} \end{bmatrix} \begin{Bmatrix} U_I \\ U_{II} \\ U_{III} \end{Bmatrix} = \begin{Bmatrix} F_I \\ F_{II} \\ F_{III} \end{Bmatrix} \quad (2.44)$$

Here the suffix I denotes the degree of freedom associated with contact nodes and the nodes at which non zero forces are specified, II denotes the degree of freedom associated with the free surface and internal nodes, while III denotes the degree of freedom associated with the nodes at which

displacements are specified. If the prescribed displacements are zero then $U_{III} = 0$. Further the nodal force at the free surface and internal nodes are zero i.e. $F_{II} = 0$. Thus the Eq. (2.44) reduces to

$$K_{I,I}\, U_I + K_{I,II}\, U_{II} = F_I \tag{2.45}$$

$$K_{II,I}\, U_I + K_{II,II}\, U_{II} = 0 \tag{2.46}$$

Eliminating U_{II} from the above equations we get

$$\overline{K_{I,I}}\; U_I = F_I \tag{2.47}$$

where $$\overline{K_{I,I}} = (K_{I,I} - K_{I,II}\, K_{II,II}^{-1}\, K_{II,I}) \tag{2.48}$$

To obtain the matrix $\overline{K_{I,I}}$, $K_{I,I}$ is first extracted in full form from the global stiffness matrix in skyline form. Next $K_{II,II}$ is obtained in skyline form from the global stiffness matrix. Then the matrix $K_{II,II}^{-1} K_{II,I}$ is obtained columnwise. If $\{ C \}_i$ is its i^{th} column, then it is obtained by solving the system

$$\left[K_{II,II} \right] \left\{ C \right\}_i = \left\{ K_{II,I} \right\}_{i^{th}\text{Column}} \tag{2.49}$$

Thus the inverse of $K_{II,II}$ is not explicitly found. Next the elements of the matrix $K_{I,II}\, K_{II,II}^{-1}\, K_{II,I}$ are obtained by multiplying the rows of $K_{I,II}$ with the appropriate column of $K_{II,II}^{-1} K_{II,I}$. In this step as well as in the earlier step, we need the matrices $K_{I,II}$ and $K_{II,I}$ (these are transpose of each other). But these matrices are not determined explicitly. Instead their rows

and columns are generated as and when required. Finally $\overline{K_{I,I}}$ is obtained using the eq. (2.48).

Substructuring thus leads to a smaller set of equations (2.47). This set is solved after applying the contact conditions. Displacements U_{II} are obtained by back substituting U_I in the quation

$$U_{II} = - K_{II,II}^{-1} K_{II,I} U_I \qquad (2.50)$$

Once all the displacements are known F_{III} can be readily found using the third set of equation (2.44).

2.3.3.4 CONTACT CONDITIONS APPLICATION PROCEDURE :

The set of equations (2.47) are solved iteratively by applying the contact conditions in the following way

(1) A set of nodal points is assumed to be in contact (it should include all possible contact points) and equations (2.47) are solved after applying the contact conditions where the fourth condition is the no slip condition, Eq.(2.42).

(2) The normal nodal forces cannot be tensile. Hence all those nodes where normal nodal forces come out to be tensile are deleted from the possible contact zone in the next iteration.

(3) The ratio of the tangential nodal force to the normal nodal force is calculated at all the nodes in contact. If this ratio is greater than the coefficient of friction between the two surfaces at any node, it implies that this node is slipping in the tangential direction relative to the corresponding contact node. For the nodes which

slip, the contact condition (2.42) is replaced by (2.43). in the next iteration. The other nodes are still governed by the condition (2.42).

The steps 2 and 3 are repeated until all the normal forces in the contact zone come out to be compressive and the ratio of the tangential force to the normal force for all the nodes in contact is either equal or less than the coefficient of friction. Once the iterations are over the stresses are computed.

2.3.4 EVALUATION OF STRESSES :

To evaluate the stress at a point, first the displacement vector $\{ u \}_{nodal}$ for the element, to which the point belongs, is obtained from the solution vector $\{ U \}$. Then the stress vector is given by the equations (2.15) and (2.23).

$$\{ \sigma \} = [D] \{ B \} \{ u \}_{nodal} \qquad (2.51)$$

In general the element nodes are the worse sampling points as far as determination of stress is concerned. This is because stresses are not continuous at the inter element boundaries.

2.3.4.1 STRESSES IN THE CONTACT REGION :

First, certain points on the contact surface which are away from the nodes are selected as sampling points. Then the state of stress at these points is determined by first considering them as a part of body A. The stress vector $\{ t \}$ at that point is given by

$$\begin{Bmatrix} t_x \\ t_z \end{Bmatrix} = \begin{bmatrix} \sigma_x & \tau_{xz} \\ \tau_{xz} & \sigma_z \end{bmatrix} \begin{Bmatrix} n_x \\ n_z \end{Bmatrix} \qquad (2.52)$$

where $\{n\} = \begin{Bmatrix} n_x \\ n_z \end{Bmatrix}$ is the unit outward normal at that point to the boundary of body A. Similarly, the stress vector $\{ t \}$ is calculated by considering the point as the part of body B. Then the actual stress vector is determined by averaging it over bodies A and B. Finally, the normal and shear components of stress are calculated as follows :

$$\sigma_n = t_x n_x + t_z n_z \qquad (2.53)$$

$$\tau = \sqrt{t_x^2 + t_z^2 - \sigma_n^2} \qquad (2.54)$$

2.3.4.2 STRESSES AT THE CORNER POINT :

For the evaluation of stress at the corner points of the neck, Gauss integration points are selected as sampling points. The stresses at a node of an element are calculated by linear interpolation of the stresses at the Gauss points. The interpolation is done as follows. Similar to the approximation of the displacement, a stress component at a Gauss point (σ_g) is approximated as a sum of the products of the shape functions (N_j) with its

nodal value $(\sigma_c)_j$

where $j = 1, 2, -- 4$. Thus at the four Gauss points $i = 1, 2, -- 4$,

$$(\sigma_g)_i = (\sigma_c)_1 (N_1)_i + (\sigma_c)_2 (N_2)_i + (\sigma_c)_3 (N_3)_i + (\sigma_c)_4 (N_4)_i \quad (2.55)$$

By inverting this set of equations, we get,

$$\begin{Bmatrix} (\sigma_c)_1 \\ (\sigma_c)_2 \\ (\sigma_c)_3 \\ (\sigma_c)_4 \end{Bmatrix} = \begin{bmatrix} (N_1)_1 & (N_2)_1 & (N_3)_1 & (N_4)_1 \\ (N_1)_2 & (N_2)_2 & (N_3)_2 & (N_4)_2 \\ (N_1)_3 & (N_2)_3 & (N_3)_3 & (N_4)_3 \\ (N_1)_4 & (N_2)_4 & (N_3)_4 & (N_4)_4 \end{bmatrix}^{-1} \begin{Bmatrix} (\sigma_g)_1 \\ (\sigma_g)_2 \\ (\sigma_g)_3 \\ (\sigma_g)_4 \end{Bmatrix}$$

..... (2.56)

This gives the stress component at all the nodes of the element. The state of stress at the corner of the neck is evaluated by averaging the stress matrix over all the adjacent elements. Finally the equivalent stress is calculated by the relation

$$\sigma_{eq} = \sqrt{\sigma_1^2 - \sigma_1\sigma_2 + \sigma_2^2} \quad (2.57)$$

where σ_1 and σ_2 are the principal stresses. This is done to simplify the expression for the Von Mises criterion. Now the criterion states that yielding occurs when,

$$\sigma_{eq} = \sigma_y \text{ , yield stress in tension.} \qquad (2.58)$$

Thus the numerical value of σ_{eq} immediately tells us whether there is yielding or not.

CHAPTER III

RESULTS AND DISCUSSION

A computer program was developed to implement the analysis presented in chapter II. The program first calculates the stresses in the blade and the disc which provide the boundary conditions for the main problem. In the second stage, the main problem - analysis of the root region as a plane stress contact problem with friction - is solved using finite element method. The program takes the following data as input :

(1) blade, disc and contact geometry

(2) material properties of the blade and the disc

(3) rotational speed of the turbine.

The output consists of

(1) stresses and displacements fields at the contact interface

(2) equivalent stress at the corner of the neck of the blade root.

The data on the material properties of the blade and disc and the turbine speed used in the computations is as follows :

Young's modulus, $E = 2 \times 10^5$ N/mm^2

Poisson's ratio, $\nu = 0.25$

coefficient of friction between the blade and disc, $\mu = 0.20$

density of the blade
and disc material, $\rho = 8 \times 10^{-6}$ Kg/mm^3
speed of the rotor = 3000 rpm

3.1 STRESSES IN THE BLADE AND DISC :

The stresses in the blade and the disc are calculated using the analysis of sections 2.1 and 2.2 respectively. The following geometrical data is used for these calculations.

outer radius of the disc, R_1 = 170 mm
inner radius of the disc, R_2 = 50 mm
length of the blade, l_b = 100 mm
distance of the cross-section
of the blade at which the
axial stress is calculated, Z = 20 mm

The axial stress on the blade cross-section, AB (Fig. 3.1) comes out to be 14.52 N/mm^2. The variation of radial and circumferential stresses in the disc with respect to the radial co-ordinate is shown in Fig. 3.2. The stress component t_x and t_y on the boundaries CD, DE and EF (refer to Fig. 3.1) are calculated from this information.

3.2 ANALYSIS OF THE ROOT REGION :

Analysis of the root region is carried out using the finite element formulation of section 2.3. Four noded isoparametric element is used. The program was tested by analysing the tee-root considered by Shrivastava (15) and comparing our results with his results. The comparison was made for the stresses and displacements only along the contact length and there was a very good agreement.

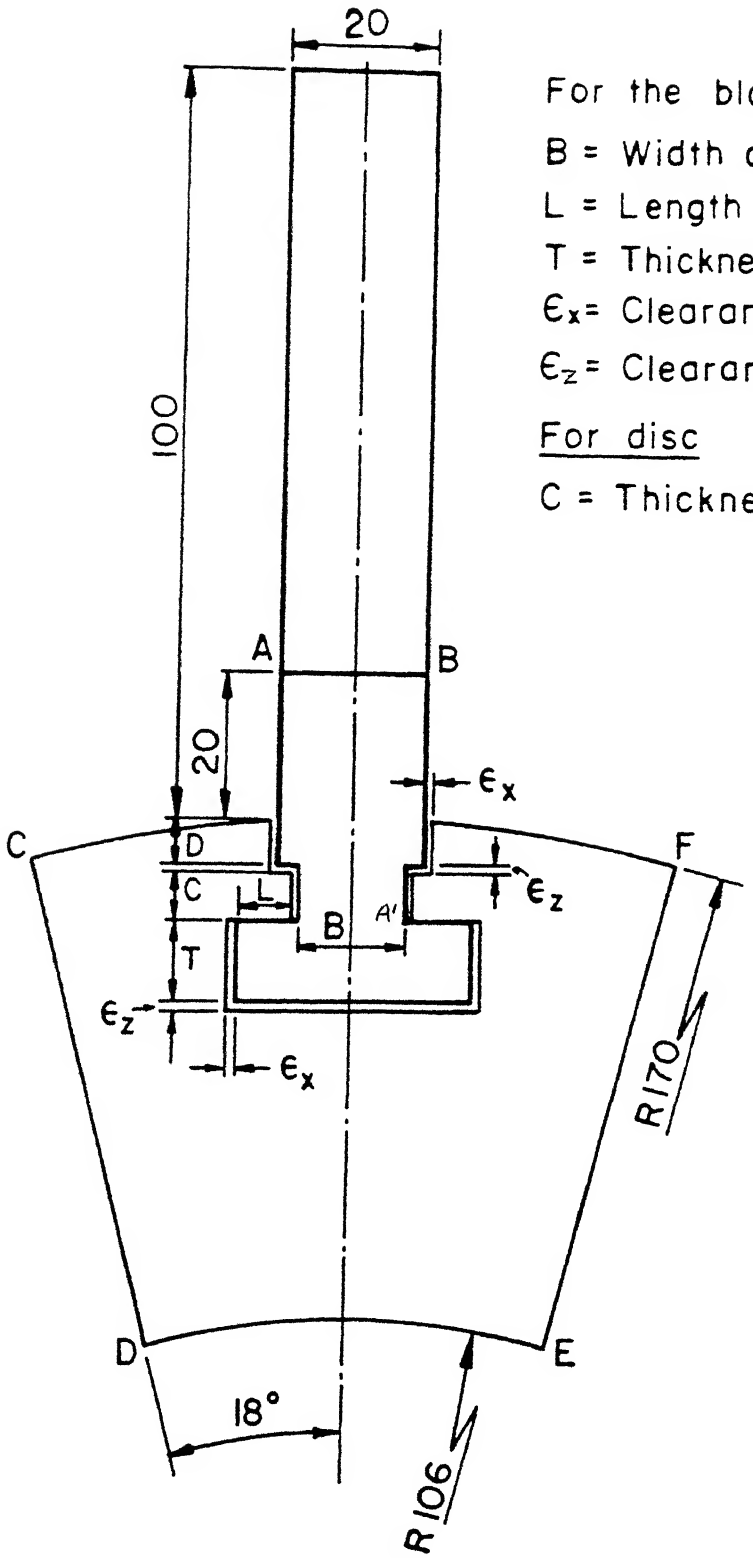

For the blade

B = Width of the k

L = Length of the shoulder

T = Thickness of the shoulder

ϵ_x = Clearance in x direction

ϵ_z = Clearance in z direction

For disc

C = Thickness of disc arm

AB and CDEF boundaries define the root domain.

Inner radius of disc = 50 mm.

Fig. 3.1 The Tee root joint between the blade and disc

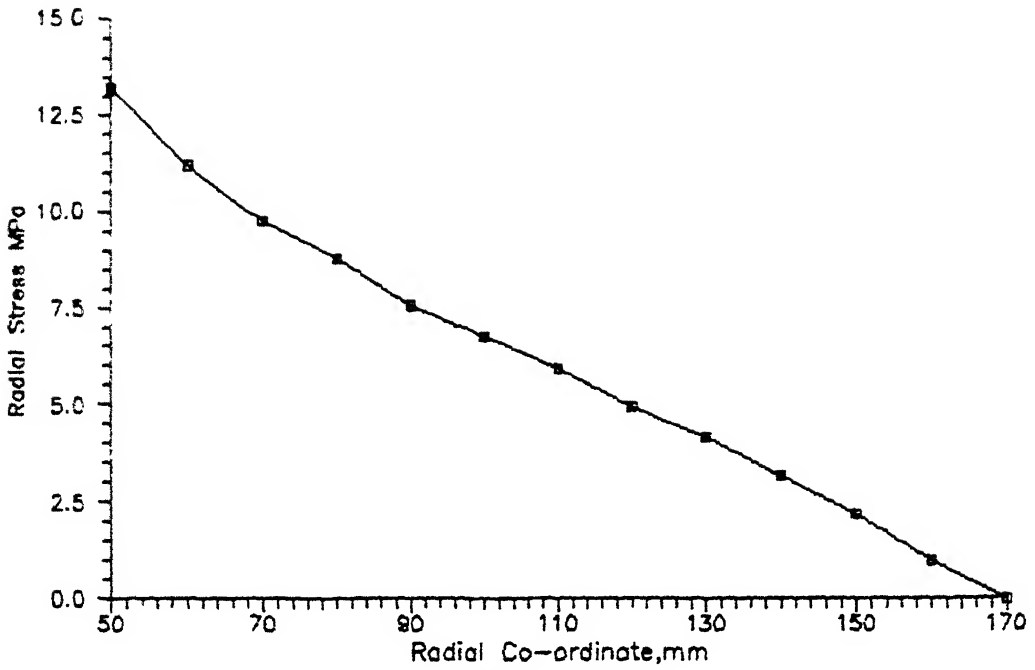

(a)

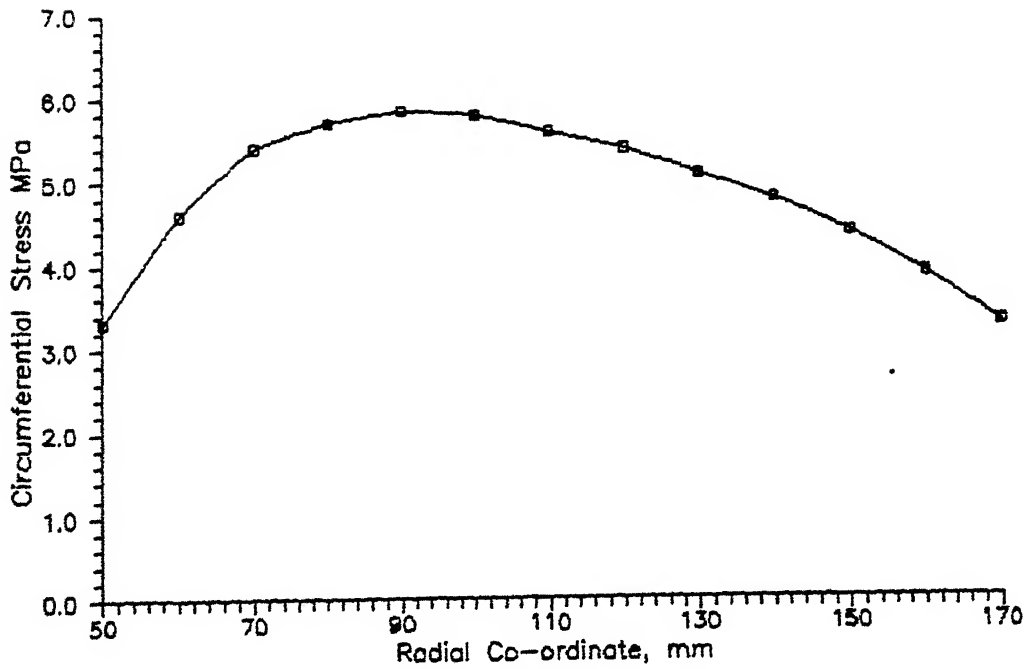

(b)

Fig. 3.2 Variation of the radial and circumferential stresses in the disc with the radial coordinate

Since no analytical or experimental results are available for the equivalent stress at the corner point, no such comparison could be made.

3.2.1 RESULTS FOR THE TEE-ROOT

The following geometric data was used in the analysis of the tee-root (see Fig. 3.1) :

B = 15 mm

C = 8 mm

D = 5 mm

L = 8 mm

ρ_x = 1 mm

ρ_z = 1 mm.

The finite element mesh used in the analysis is shown in Fig. 3.3. For the tee-root the euivalent stress σ_{eq} was calculated at the corner point A' (shown in Fig. 3.1) for the values of T/L varying from 0.75 to 1.75. This was done keeping the value of L constant. The variation of σ_{eq} with T/L is shown in Fig. 3.4. The graph shows that the equivalent stress decreases with the increase in the value of T/L. This can be explained as follows. One can consider the shoulder as a cantilever beam subjected to distributed transverse load. When T/L is increased keeping L constant it means thickness of the shoulders is increased. This increases its section modulus. Although the distribution of the transverse load may vary with T/L, total load remains the same. Therefore the change in bending moment at the corner A' may not be as prominent as the change in section modulus with T/L. Since the section modulus increases with T/L, the bending

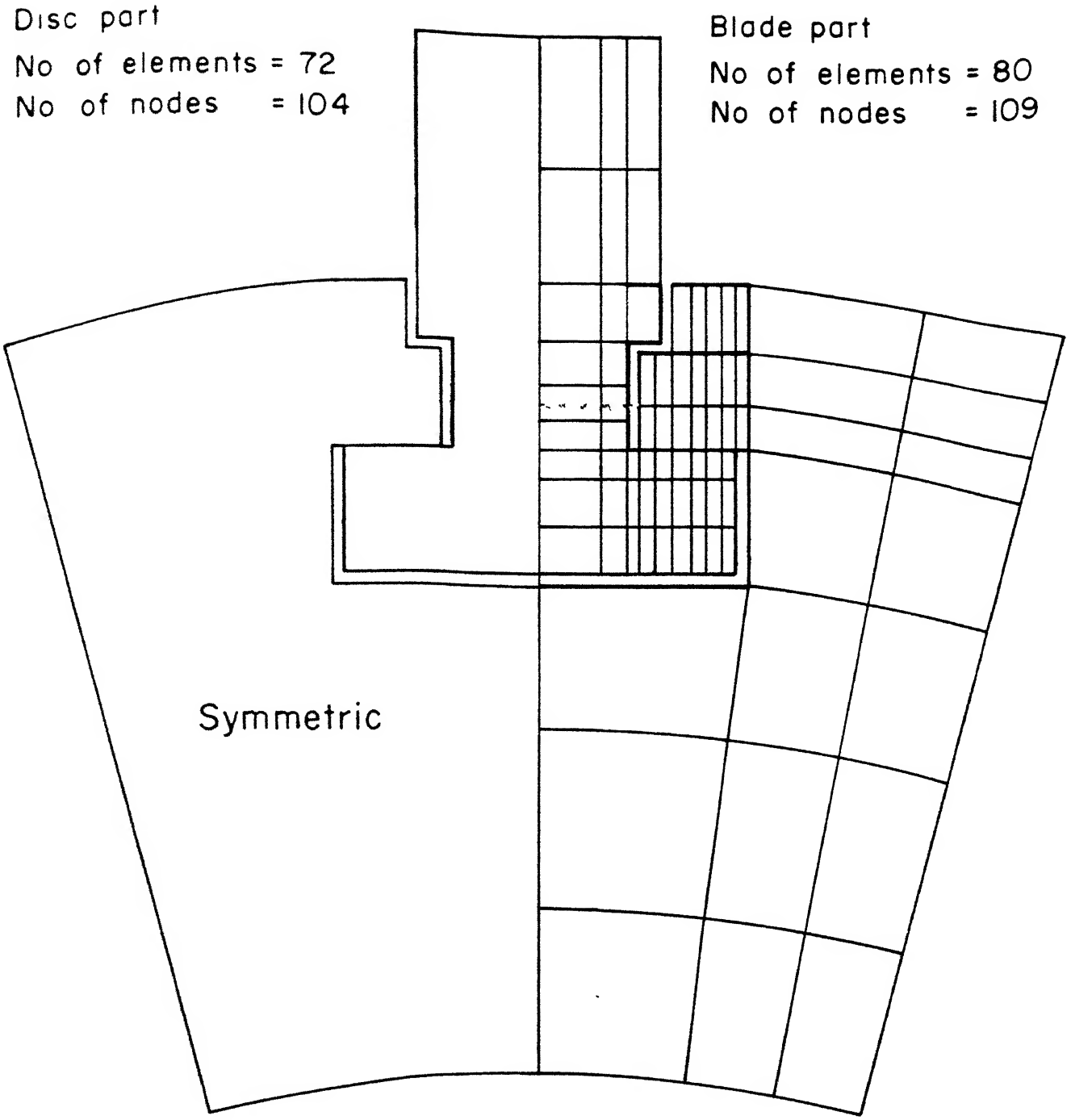

Fig. 3.3 Finite Element Mesh for Tee-Root Joint.

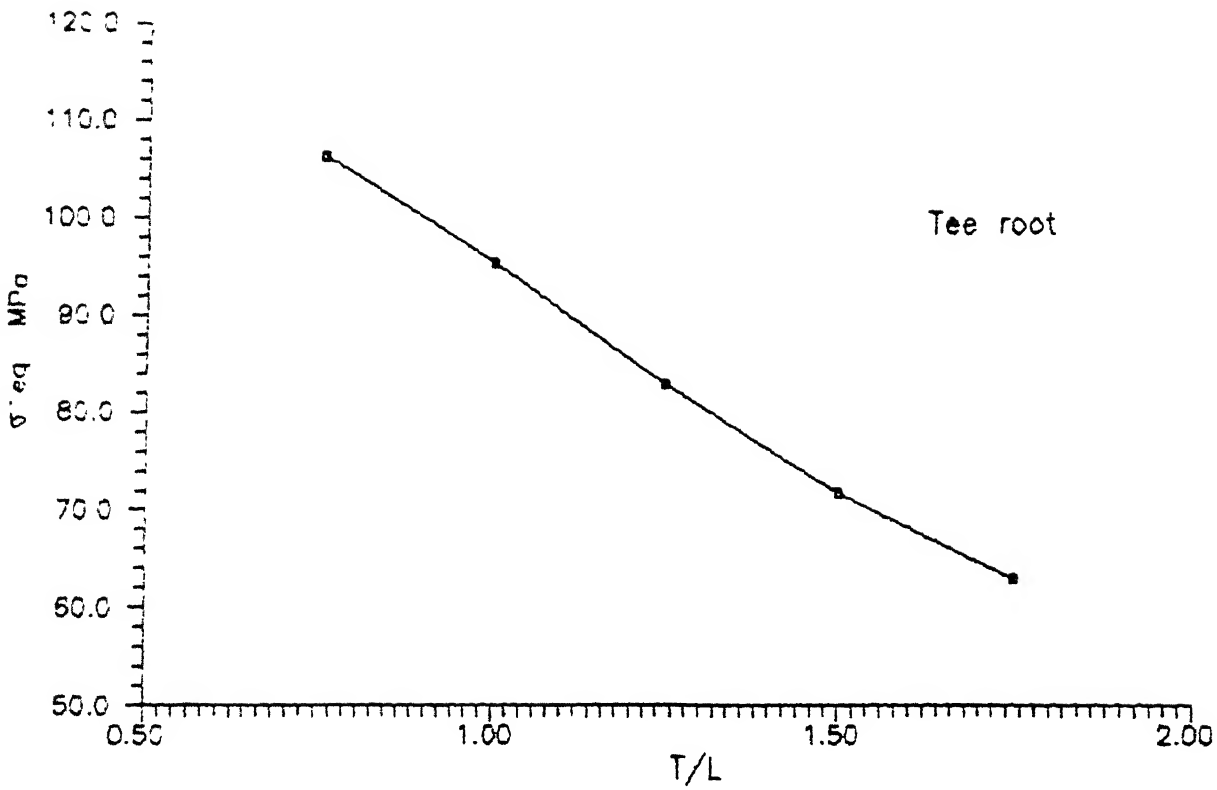

Fig. 3.4 Variation of equivalant stress at the corner with respect to thickness to length ratio

stress would decrease. Although σ_{eq} is not equal to the bending stress, it is quite possible that σ_{eq} increases whenever bending stress increases. Thus the trend of Fig. 3.4 seems quite reasonable.

3.2.2 RESULTS FOR THE STRADDLE ROOT :

Fig. 3.5 shows the geometry of the straddle root joint. The relations of various geometric parameters of the straddle root with the tee root are defined by eq.(1.1). These relations are reproduced here for the sake of convenience.

$$\left.\begin{aligned} & l_1 + l_2 = L \\ & t_1 + t_2 = T \qquad \text{where} \quad \frac{t_1}{l_1} = \frac{t_2}{l_2} \\ & c_1 + c_2 = C \qquad \text{where} \quad \frac{c_1}{l_1} = \frac{c_2}{l_2} \\ & \varepsilon_{x_1} + \varepsilon_{x_2} = \varepsilon_x \qquad \text{where} \quad \frac{\varepsilon_{x_1}}{l_1} = \frac{\varepsilon_{x_2}}{l_2} \\ & \varepsilon_{z_1} + \varepsilon_{z_2} = \varepsilon_z \qquad \text{where} \quad \frac{\varepsilon_{z_1}}{l_1} = \frac{\varepsilon_{z_2}}{l_2} \end{aligned}\right\} \qquad (3.1)$$

As stated earlier, two different models of the straddle root are considered. In the first model thicknesses of both the necks are equal i.e. $b_1 = b_2$. In the second model the thickness of the lower neck is related to that of the first by the relation

$$\frac{b_1}{b_2} = \frac{L}{l_2} .$$

Finite element mesh used in this analysis is shown in Fig. (3.6a) and (3.6b).

For the straddle root the variation of the equivalent stress at the corner points A' and B' (shown in Fig. 3.5) with respect to the ratio l_1/l_2 of the shoulder lengths was determined. This was done for various values of T/L. As l_1/l_2 increases, the length as well as the thickness of the upper shoulder increases while for the lower shoulder these dimensions decrease. If these shoulders are considered as cantilever beam subjected to transverse distributed loads, then increase of l_1/l_2 results in the increase of the section modulus of the upper shoulder but decrease in that of lower shoulder. It is possible that the bending moments at the corner A' and B' change with respect to l_1/l_2. However, the effect of the section modulus seems more dominant. Thus the bending stress and along with it the equivalent stress seems to decrease for the case of upper shoulder (point A'). For the lower shoulder (point B') it seems to increase. This trend is depicted in Figures (3.7) to (3.11). These graphs show the variation of the equivalent stresses at the two corners with respect to the ratio of shoulder lengths for five different values of T/L. The (a) part of the figure corresponds for the first model ($b_1 = b_2$) while the (b)

AB and CDEF boundaries define the blade and disc straddle

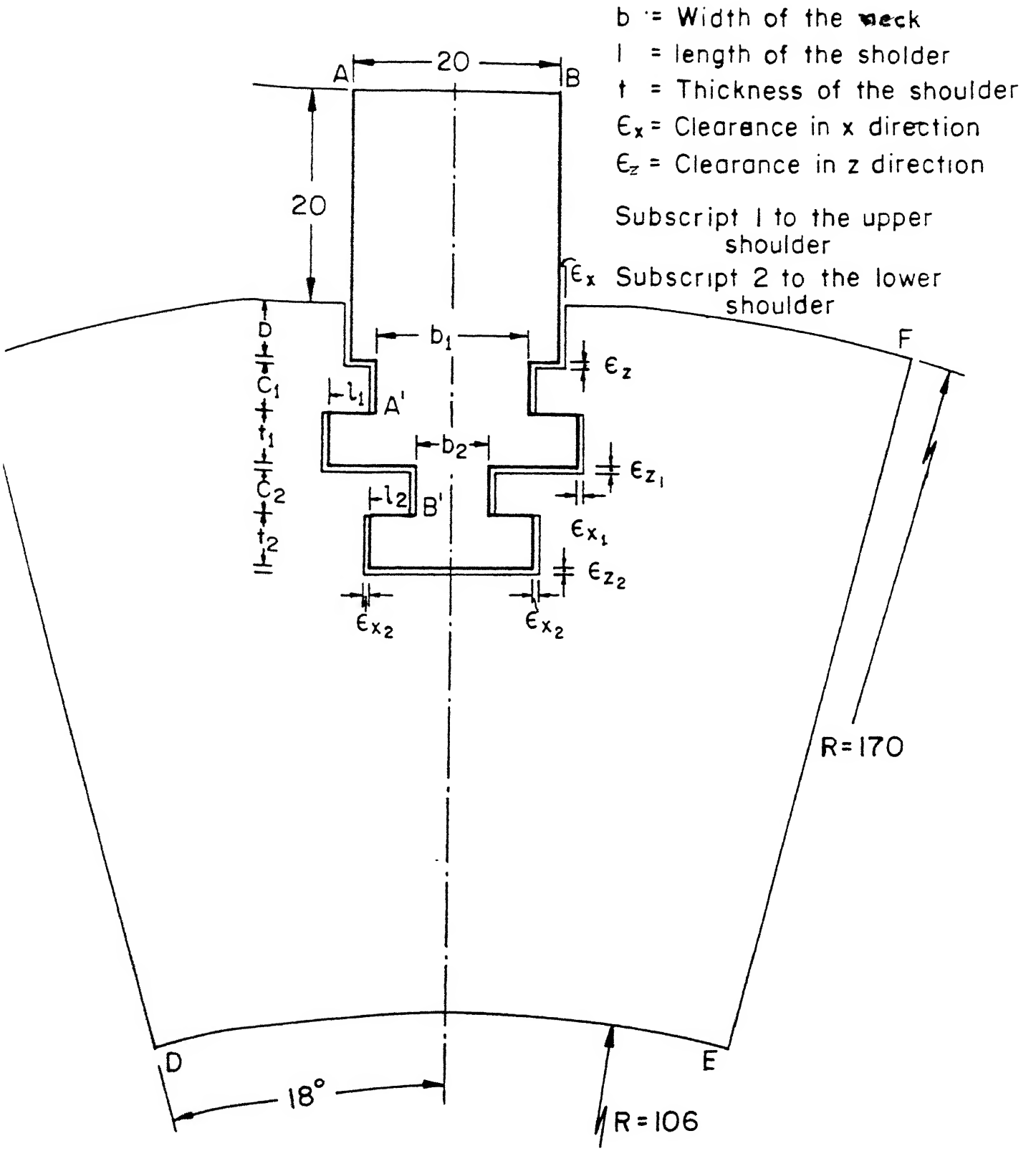

Fig 3.5 Straddle root joint between the blade and disc

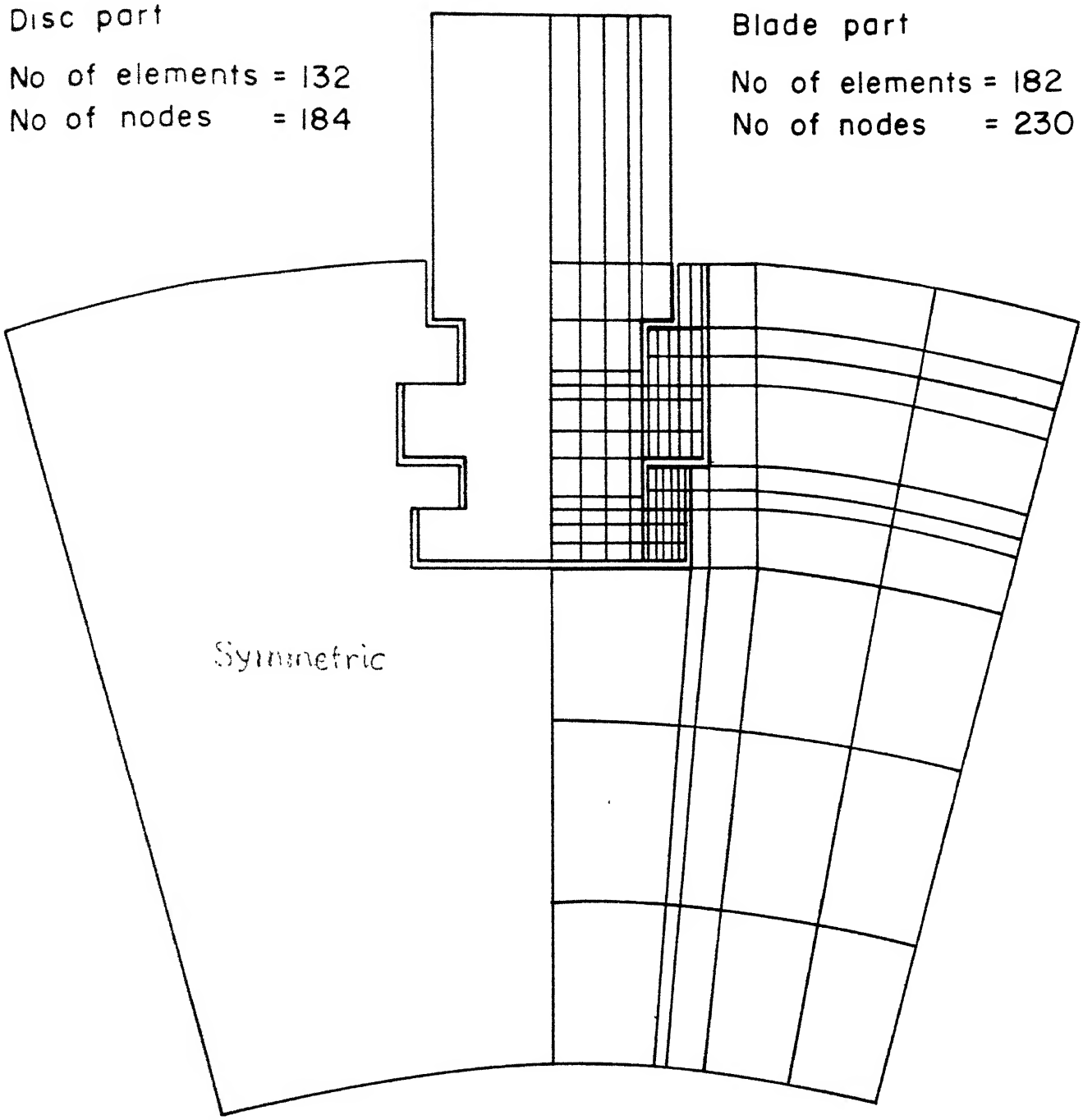

Fig 3.6(a) Finite Element Mesh for Straddle Root Contact
(Model I $b_1 = b_2 = B$)

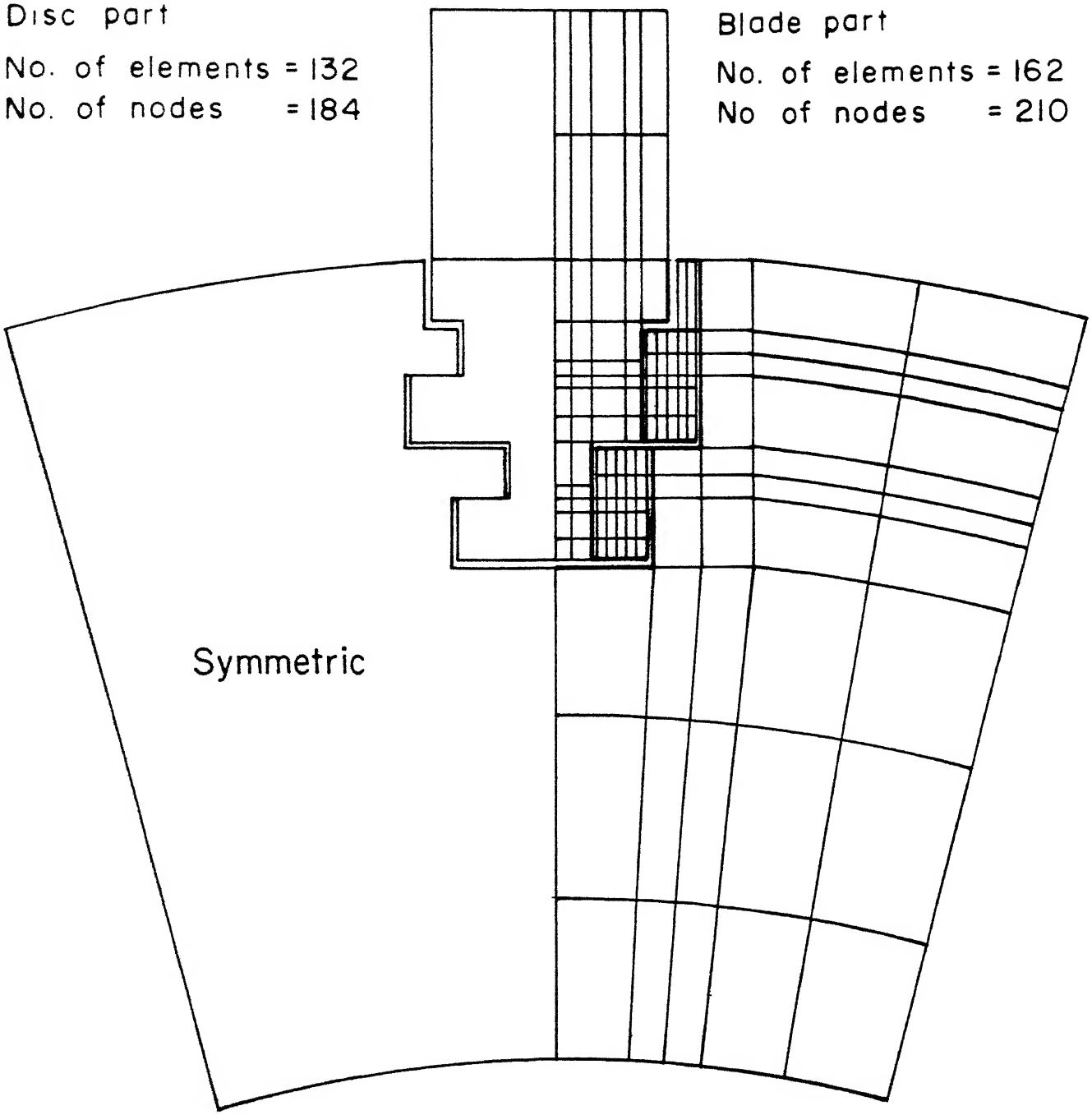

Fig.3.6(b) Finite Element Mesh for Straddle root contact
(Model II $b_1/b_2 = L/l_2$)

part corresponds to the second model ($b_1/b_2 = l_1/l_2$).

The Figures 3.7 to 3.11 indicate the optimum value of l_1/l_2 which is denoted by $(l_1/l_2)_{opt}$. It is the value at which the equivalent stresses at the corner points become equal. For the given value of T/L, $(l_1/l_2)_{opt}$ is lower for the second model. This means, in the optimum design, the second model has longer and thicker lower shoulder compared to the first model. This is probably required to compensate for the lower length of the lower neck of the second model. It may be recalled that the lower neck of the second model is thinner compared to the first model. The value of equivalent stress in the tee-root of the same T/L ratio is also indicated in the Figures (3.7) to (3.11). Figure (3.12) shows the variation of equivalent stress in the optimum straddle root with respect to T/L ratio. The variation shows the same trend as that of the tee-root. The values in the parenthesis indicate the value of $(l_1/l_2)_{opt}$. It may be noted that, for given T/L ratio the second model has higher equivalent stress compared to the first model.

3.2.3 COMPARISION OF THE TEE AND OPTIMUM STRADDLE ROOT

First we define the nondimensional equivalent stress in the optimum straddle root as follows :

$$(\bar{\sigma}_{eq})_{opt} = \frac{[(\sigma_{eq})_{opt}]_s}{(\sigma_{eq})_T}$$

where $(\bar{\sigma}_{eq})_{opt}$ = non-dimensional equivalent stress in the optimum straddle root

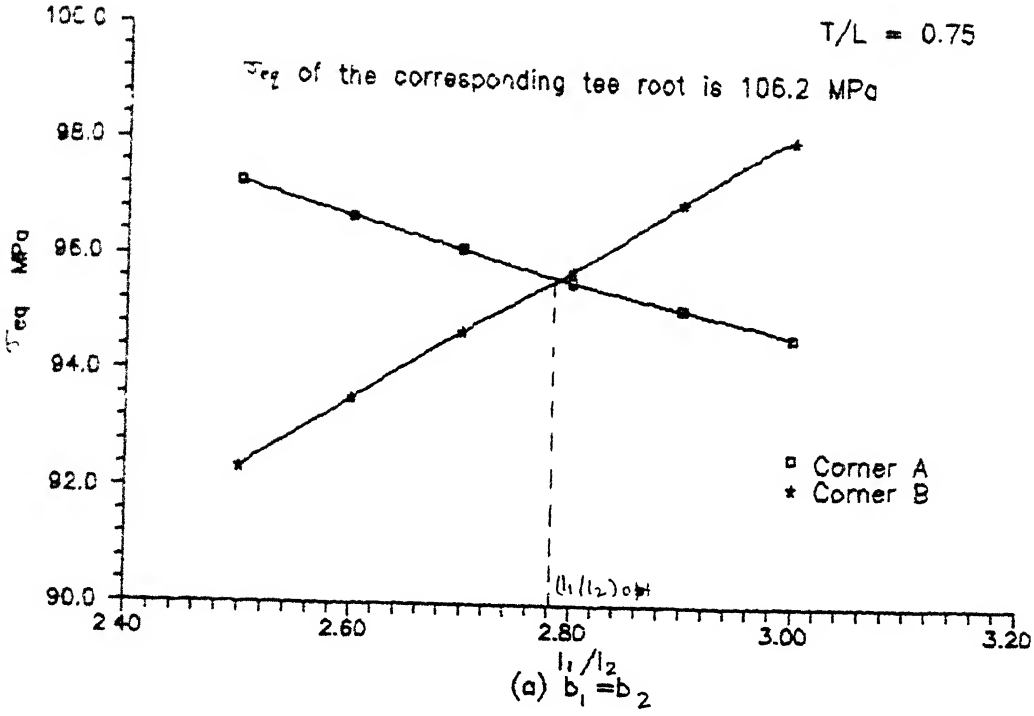

(a) $b_1 = b_2$

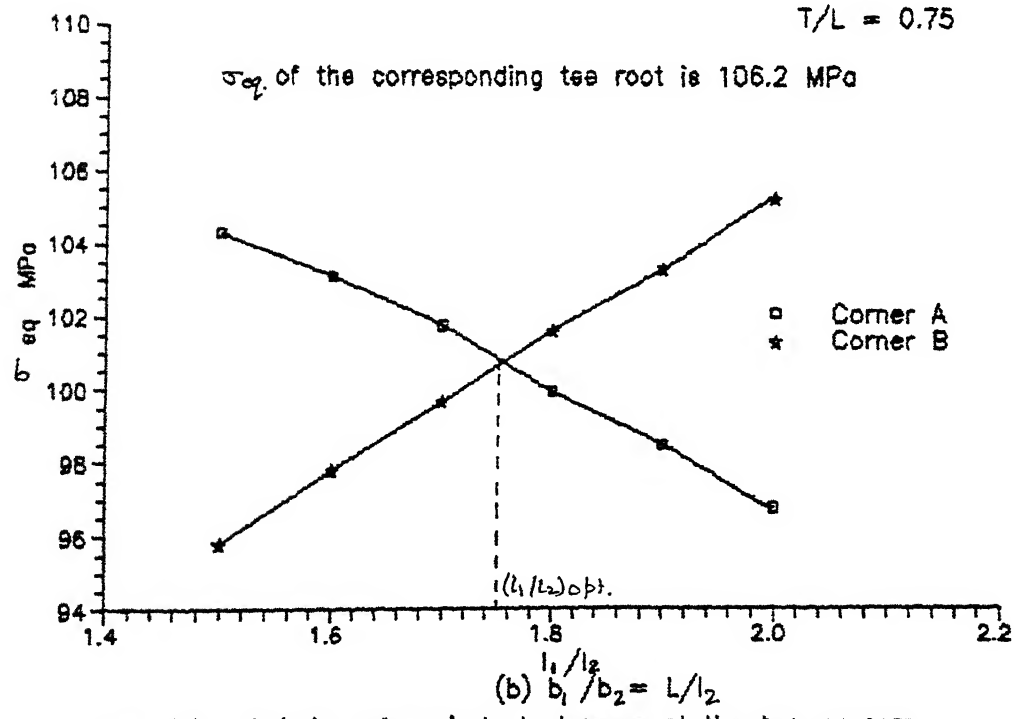

(b) $b_1/b_2 = L/l_2$

Fig. 3.7 Variation of equivalant stresses at the two corners with respect to the shoulder lengths

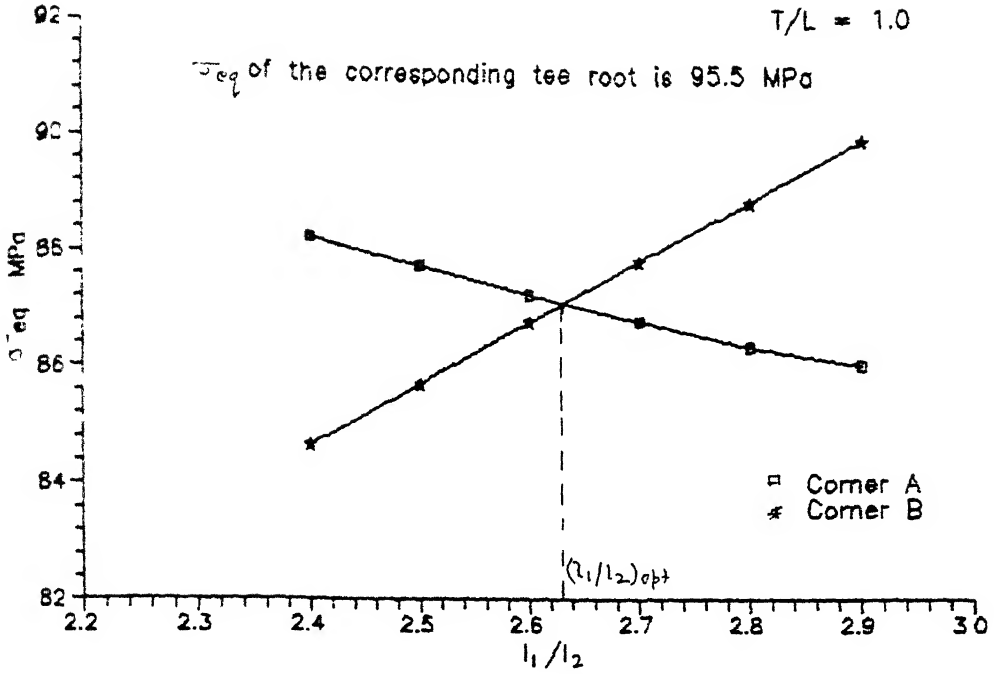

(a) $b_1 = b_2$

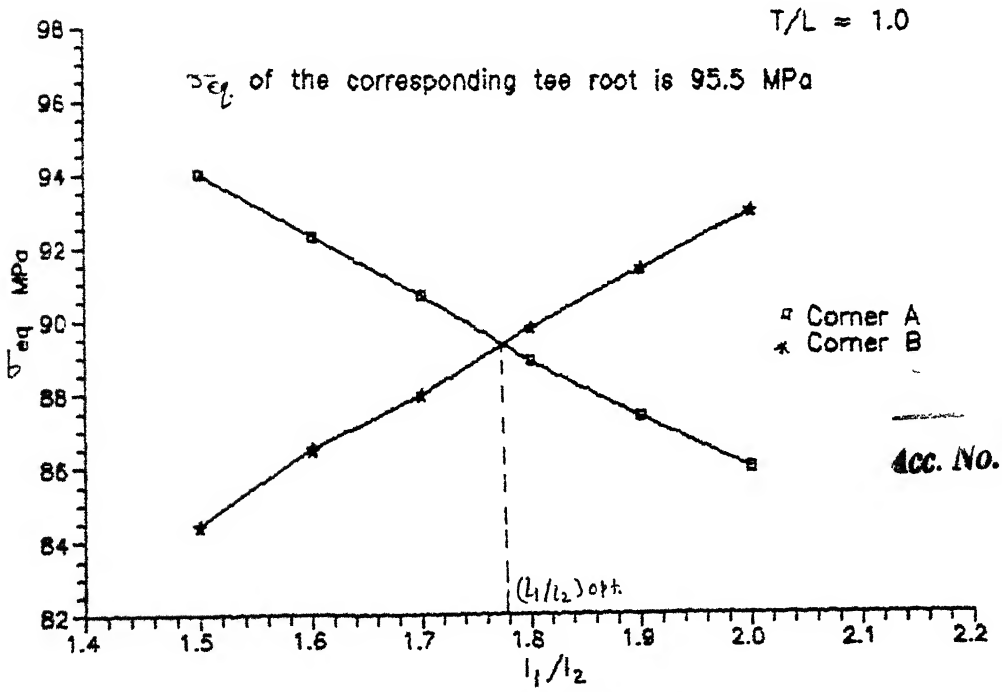

(b) $b_1/b_2 = L/l_2$

Fig.3.8 Variation of the equivalent stress at the two corners with respect to the ratio of the shoulder lengths.

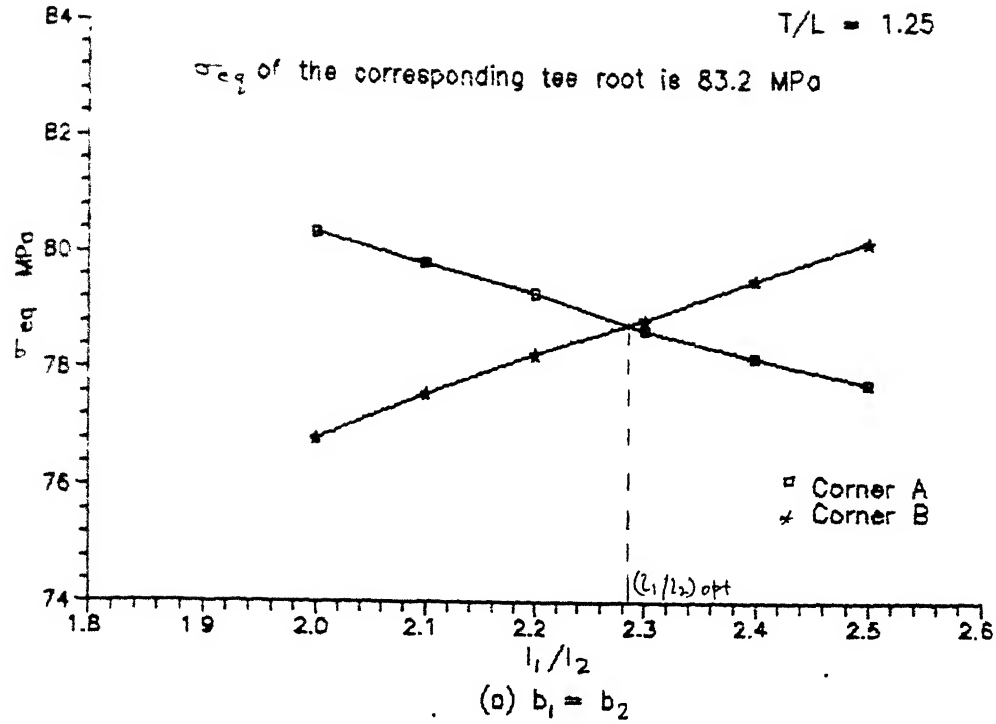

(a) $b_1 = b_2$

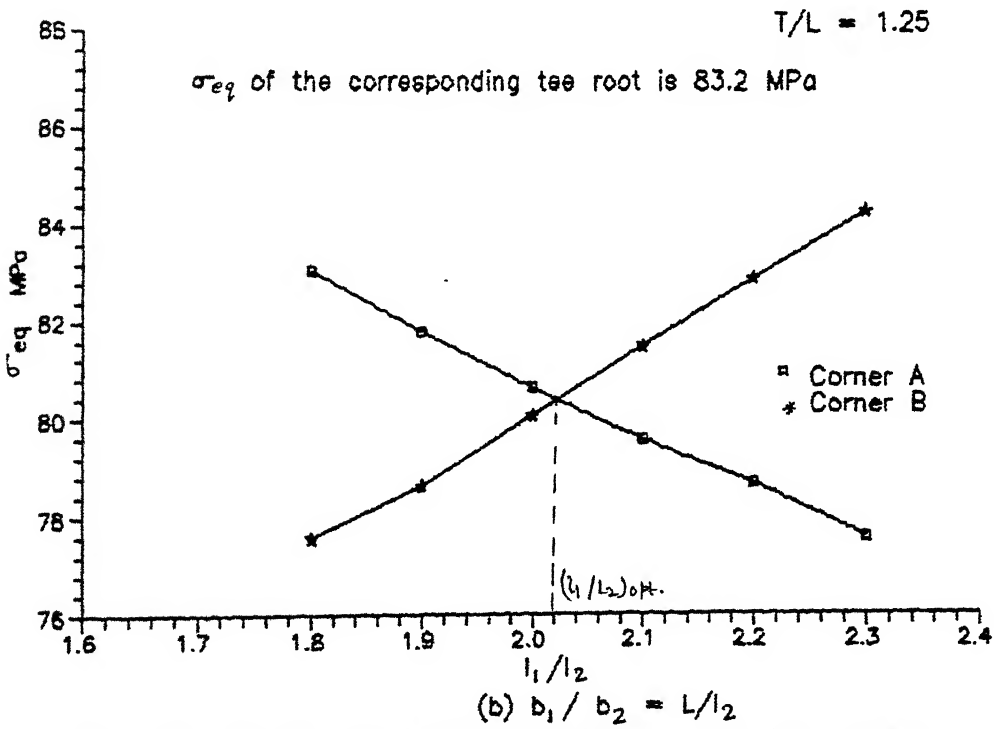

(b) $b_1 / b_2 = L/l_2$

Fig. 3.9 Variation of the equivalent stress at the two corners with respect to the ratio of the shoulder lengths→→→→→→

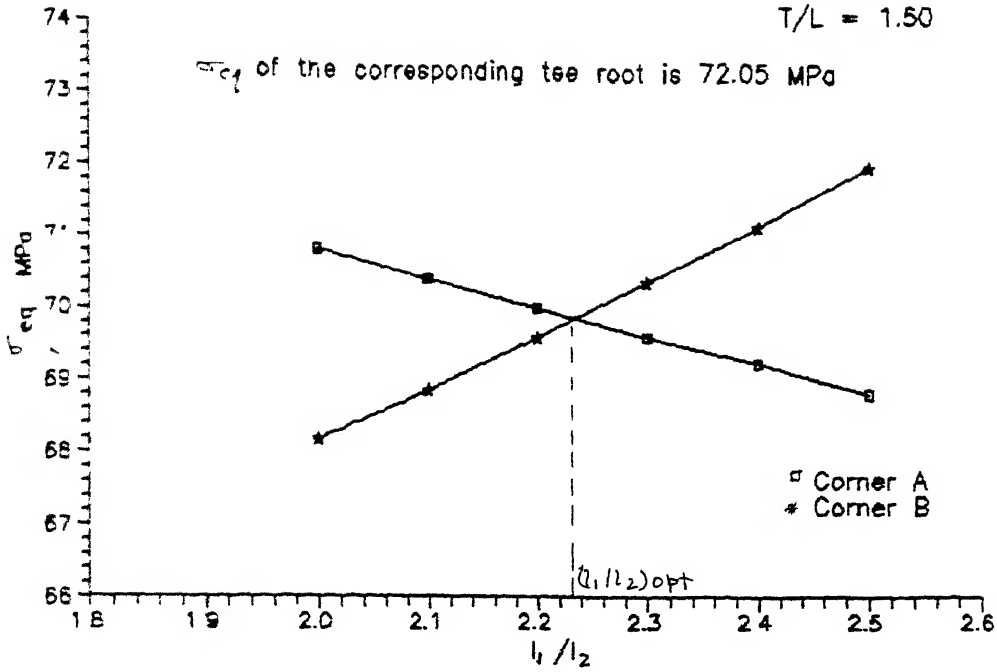

(a) $b_1 = b_2$

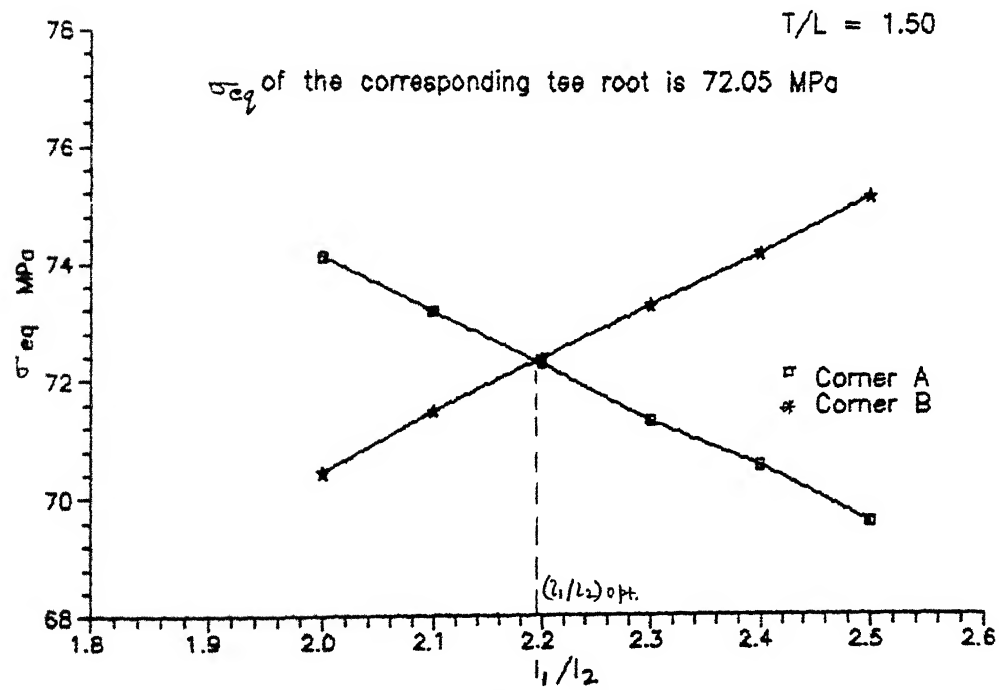

(b) $b_1 / b_2 = L/l_2$

Fig.3.10 Variation of the equivalent stress at the two corners with respect to the ratio of the shoulder lengths→→→→→→

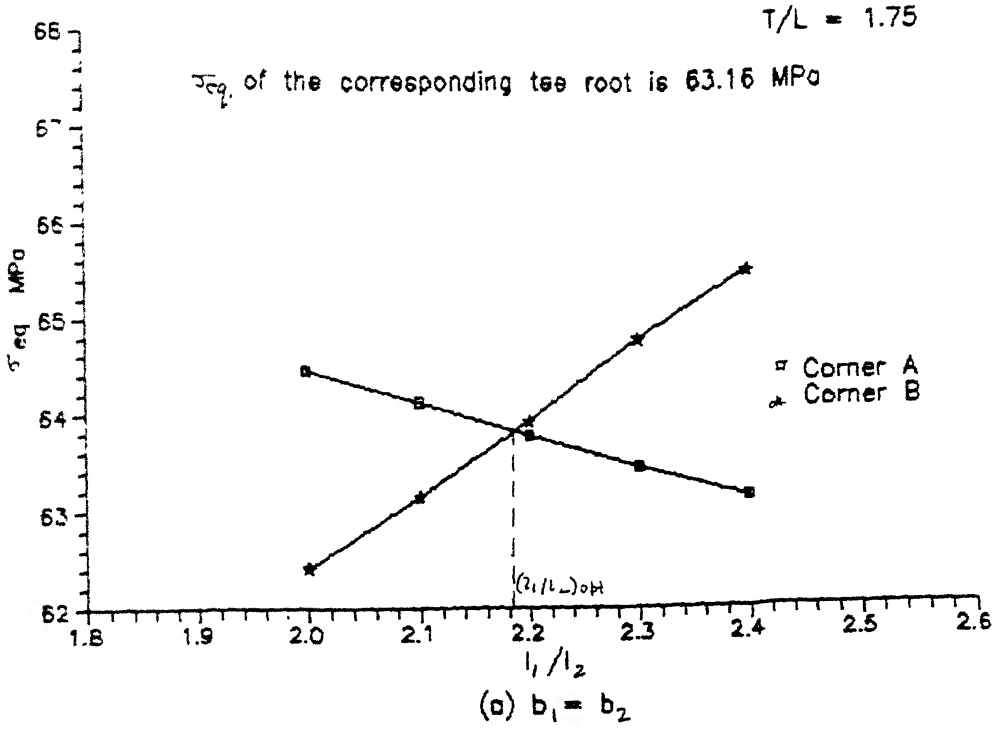

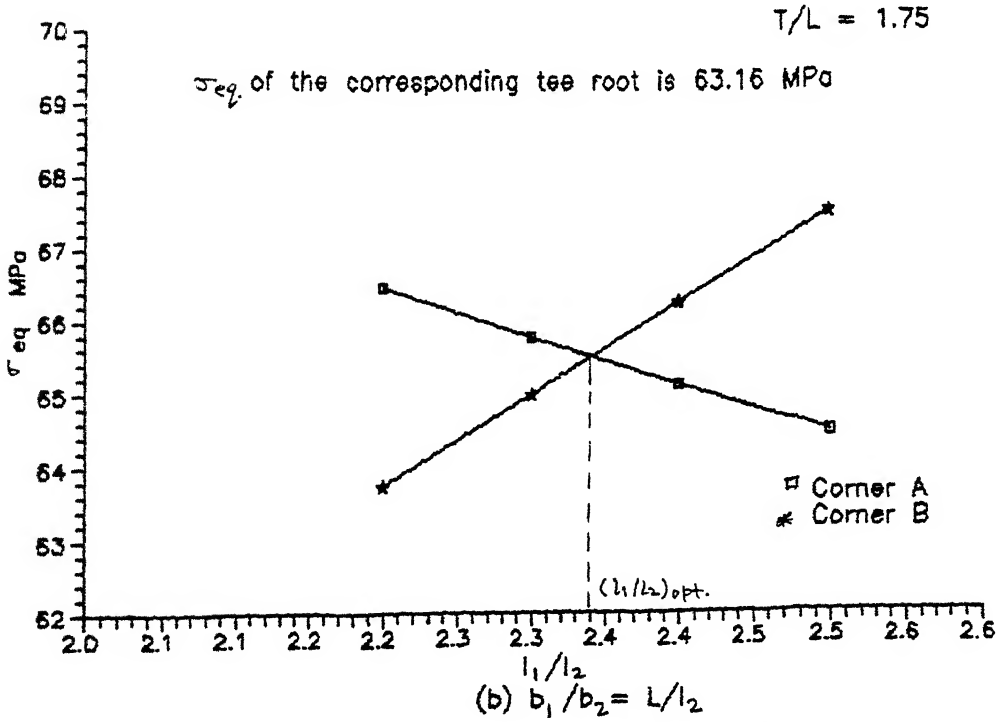

Fig.3.11 Variation of the equivalent stress at the two corners with respect to the ratio of the shoulder lengths-

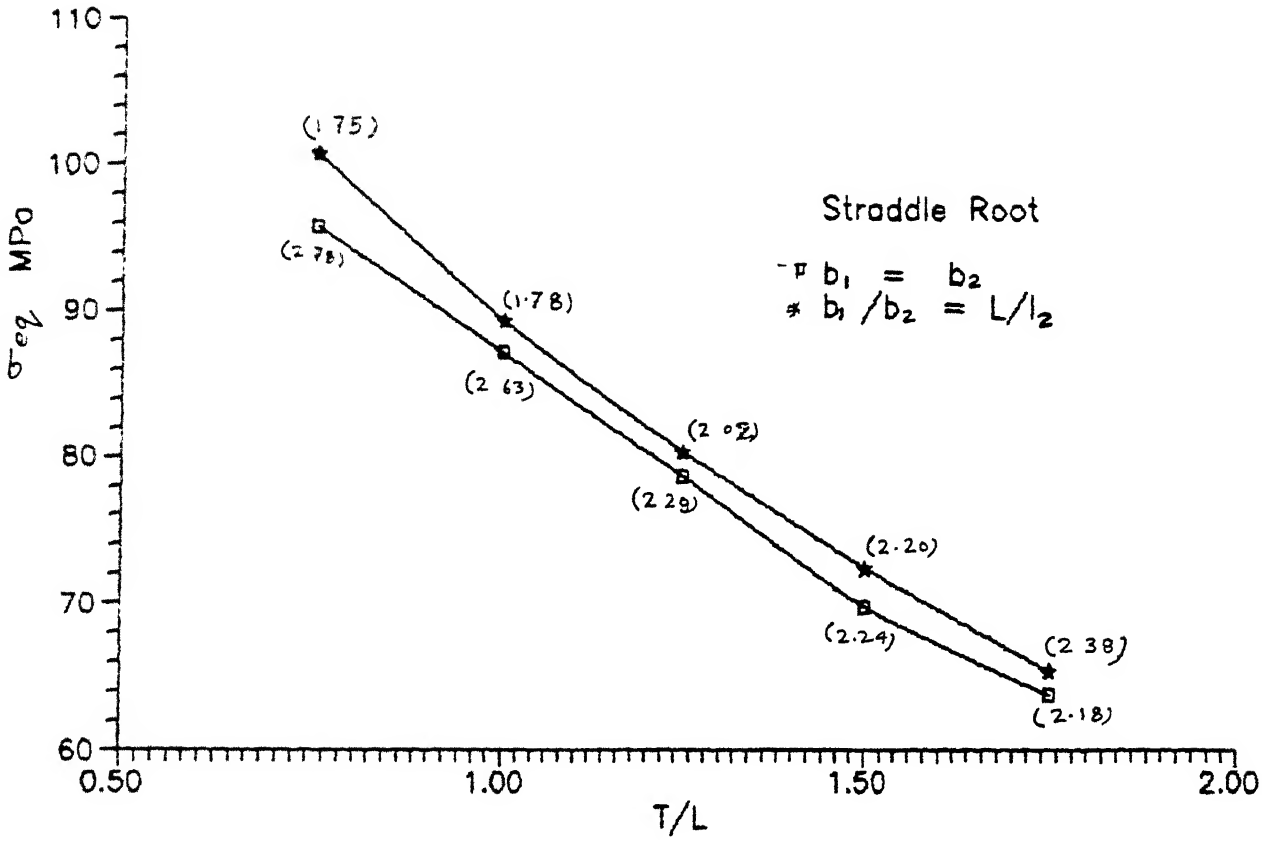

Fig.3.12 Variation of the equivalent stress in the optimum straddle root with respect to T/L ratio

$[(\sigma_{eq})_{opt}]_S$ = equivalent stress in the optimum straddle root

$(\sigma_{eq})_T$ = equivalent stress in the tee-root having the same T/L ratio.

Variation of $(\bar{\sigma}_{eq})_{opt}$ with respect to T/L ratio is shown in the Fig. (3.13). The (a) part of the figure corresponds to the first model while the (b) part corresponds to the second model. The figures are divided into two regions. In the region I, $(\bar{\sigma}_{eq})_{opt}$ is less than 1. Therfore for T/L ratios lying in this region, it is advantageous to use the optimum straddle root rather than tee root. This is because it is subjected to lower equivalent stress compared to the tee-root of the same T/L ratio. In the region II, $(\bar{\sigma}_{eq})_{opt}$ is greater than 1. This means for T/L ratios lying in this region, the tee-root has less value of equivalent stress compared to the optimum straddle root of the same T/L ratio. Therefore in this region, it is more advantageous to use the tee-root. It should be kept in mind that this comparison is only from the strength point of view and that too only for steady conditions.

3.2.4 CONTACT STRESSES AND DISPLACEMENTS :

To show a typical variation of the contact stresses and displacements, the value of T/L = 0.75 is chosen. At this value, the non-dimensional equivalent stress in the optimum straddle root is minimum. Figures 3.14 to 3.17 show respectively the variation of normal

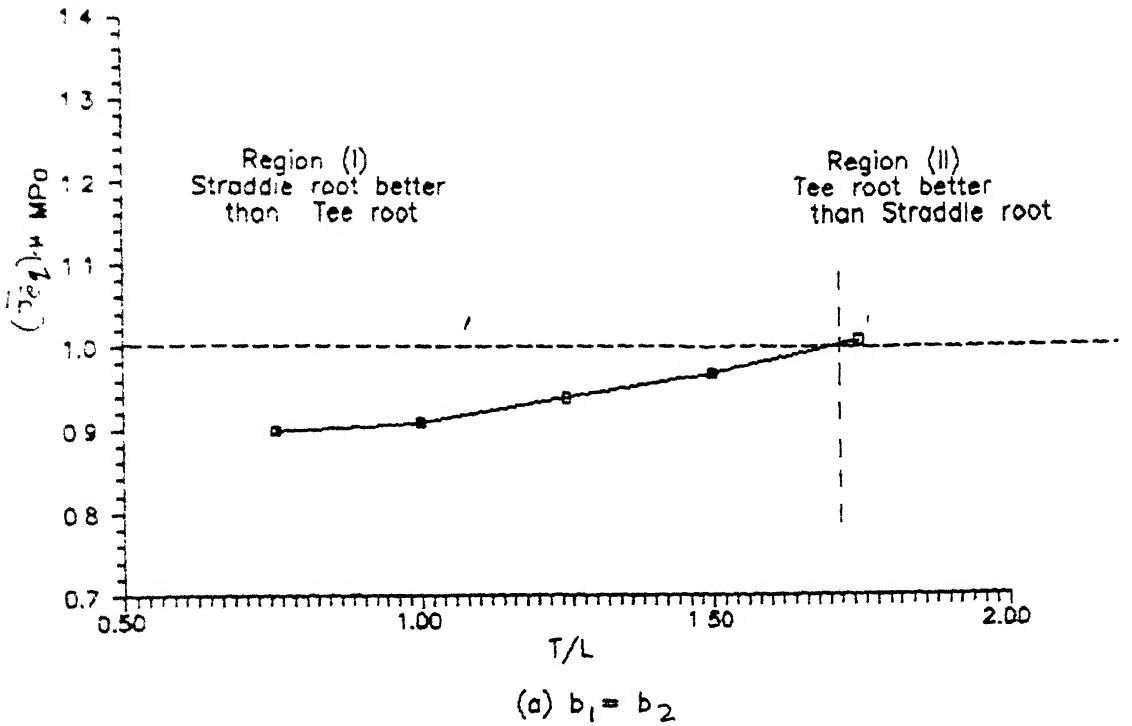

(a) $b_1 = b_2$

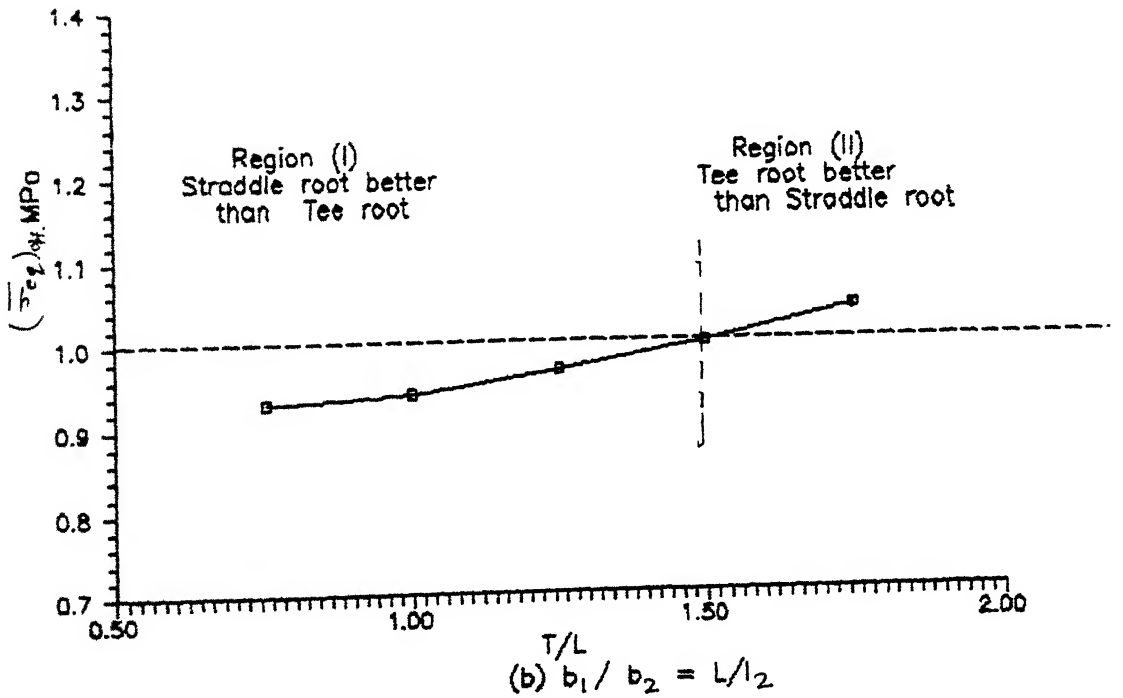

(b) $b_1 / b_2 = L/l_2$

Fig.3.13 Variation of non dimensional equivalent stress in the optimum straddle root with respect to T/L

displacement, tangential displacement, normal stress and the tangential stress along the contact length for the tee-root. Figures 3.18 to 3.21 shows the variation of the same quantities for the first model of the optimum straddle root while the Figures 3.22 to 3.25 are for the second model. In the last two sets of figures, part (a) denotes the variation along the upper shoulder while part (b) is for the lower shoulder. In all three figures, X denotes the distance of the contact point from the axis of symmetry (Z-axis). These figures show the variation only for the right hand side contact surface, the normal stress and displacements are symmetric while the tangential stress and displacements are antisymmetric.

The trend for the tee-root as well as both the models of the optimum straddle root are similar. It is observed that the normal displacement decreases as we go away from the Z-axis. This indicates that the pull of the blade is more dominant nearer the Z-axis. This seems reasonable. Similarly the normal stress also decreases as we move away from the Z-axis. This can be explained as follows. For T/L = 0.75, thickness of the disc arm is more than the thickness of the shoulder (see Fig. 3.1). This makes the disc arm more stiff compared to the shoulder. Therefore the free end of the disc arm while deflecting applies more force on the shoulder on the disc arm. Tangential displacement increases as we go away from the Z-axis. The results on the tangential stresses don't appear to be very reliable although they roughly seem to

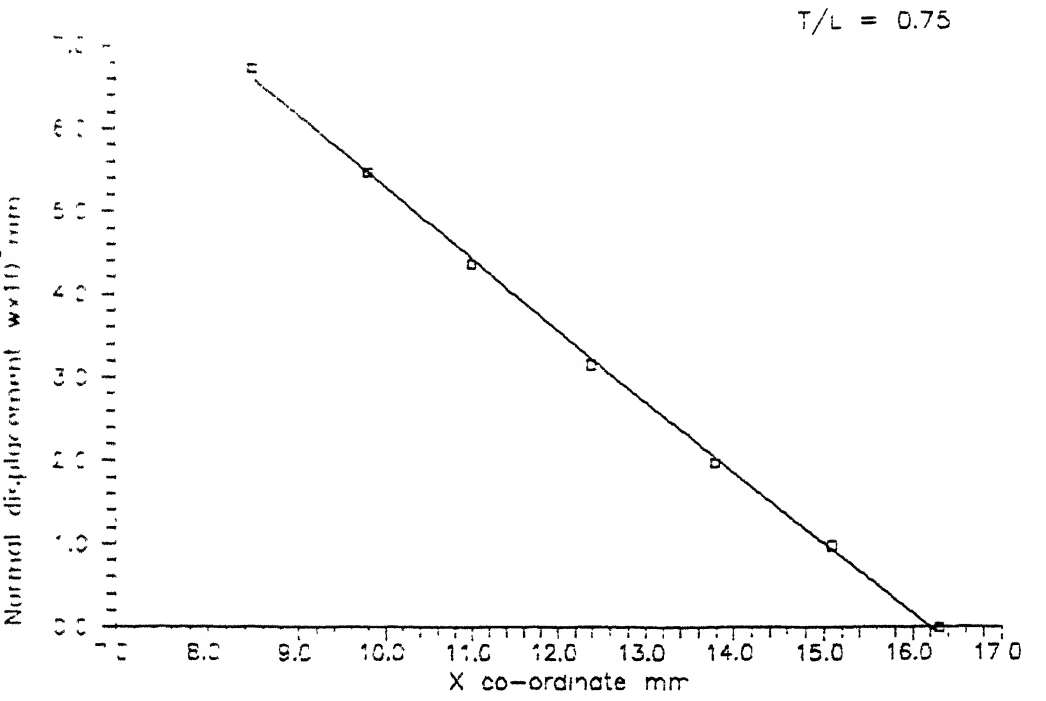

Fig 3.14 Variation of the normal displacement along the contact length (for Tee root)

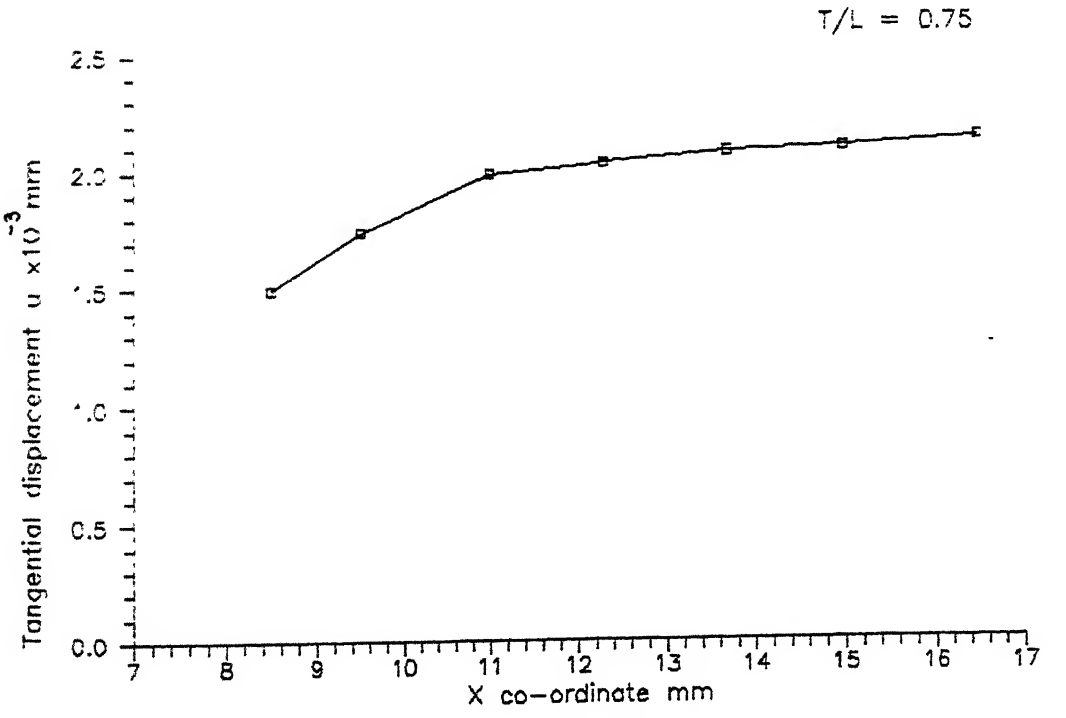

Fig 3.15 Variation of the Tangential Displacement along the contact length (for Tee root)

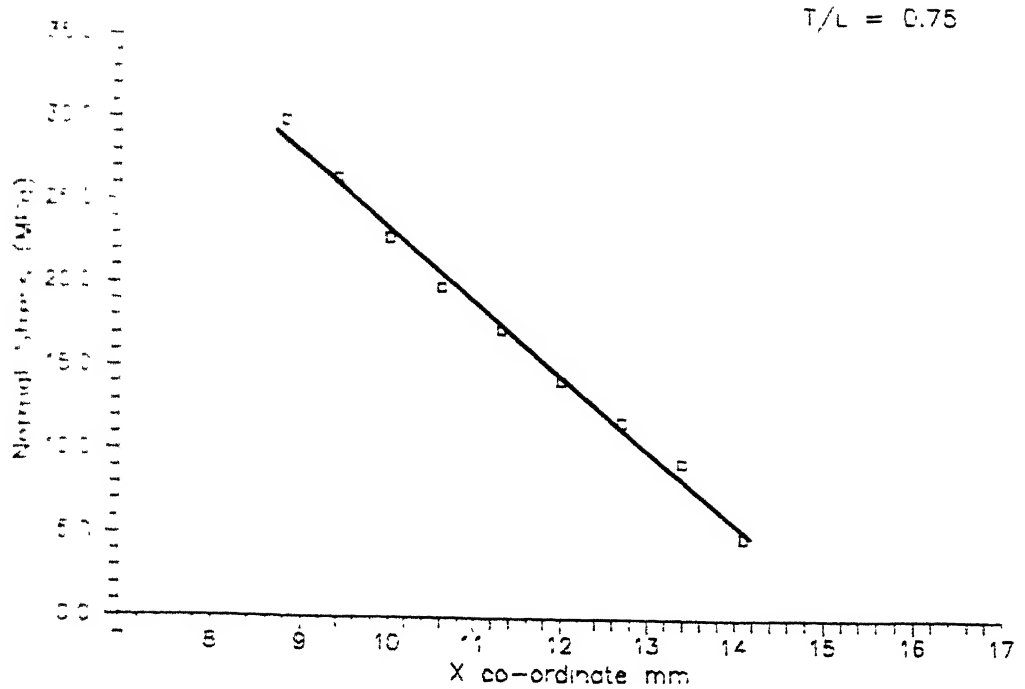

Fig 3.16 Variation of the normal stress along the contact length (for Tee root)

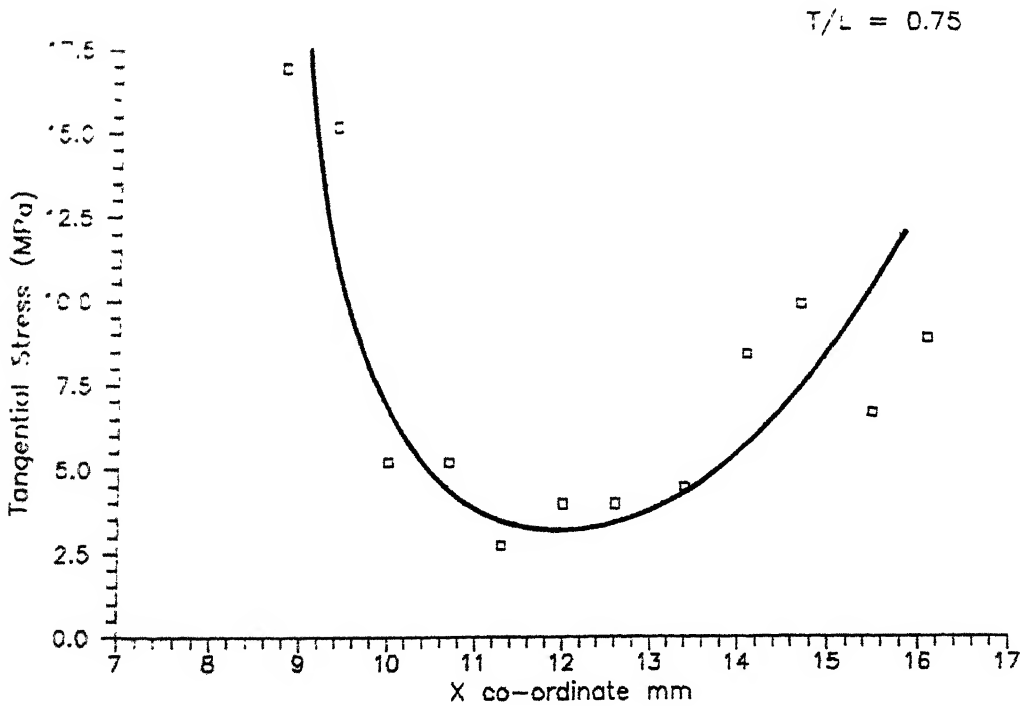

Fig 3.17 Variation of the Tangential Stress along the contact length (for Tee root)

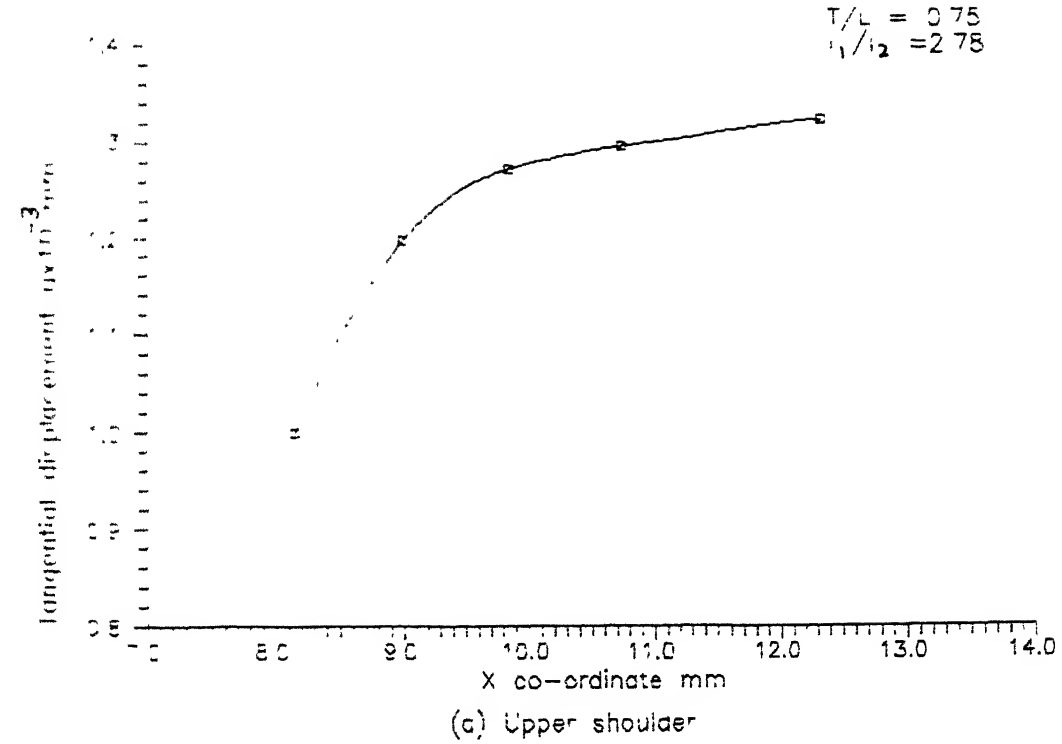

(a) Upper shoulder

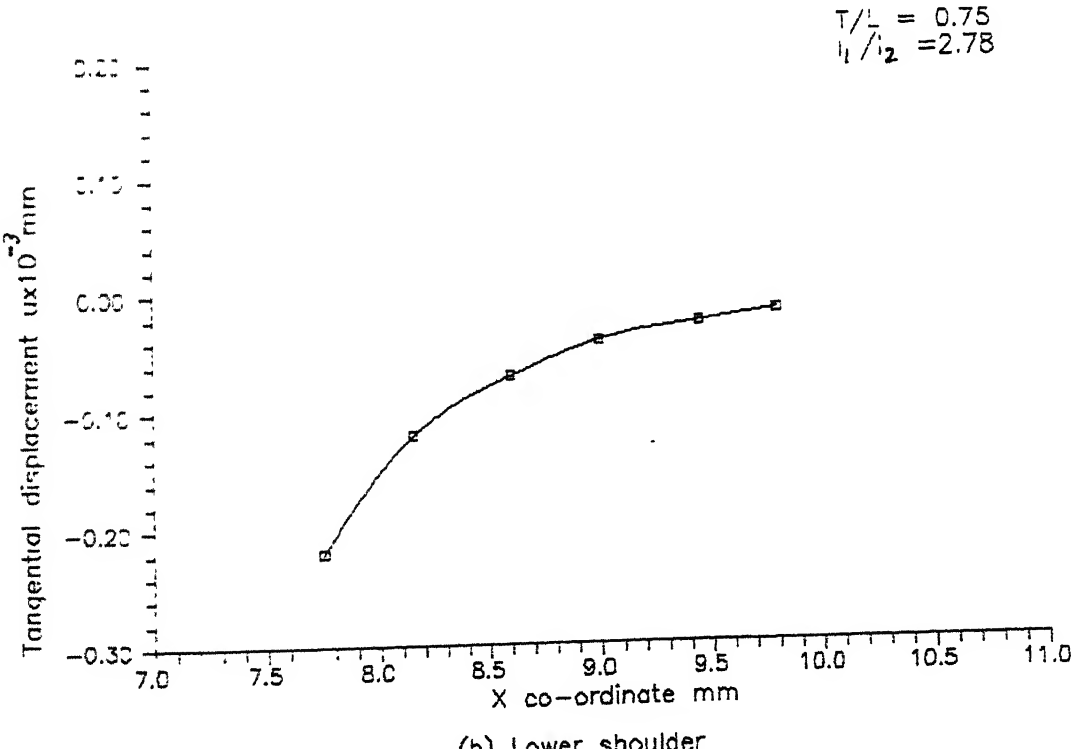

(b) Lower shoulder

Fig.3.19 Variation of tangential displacement along the contact length (for straddle root, model I)

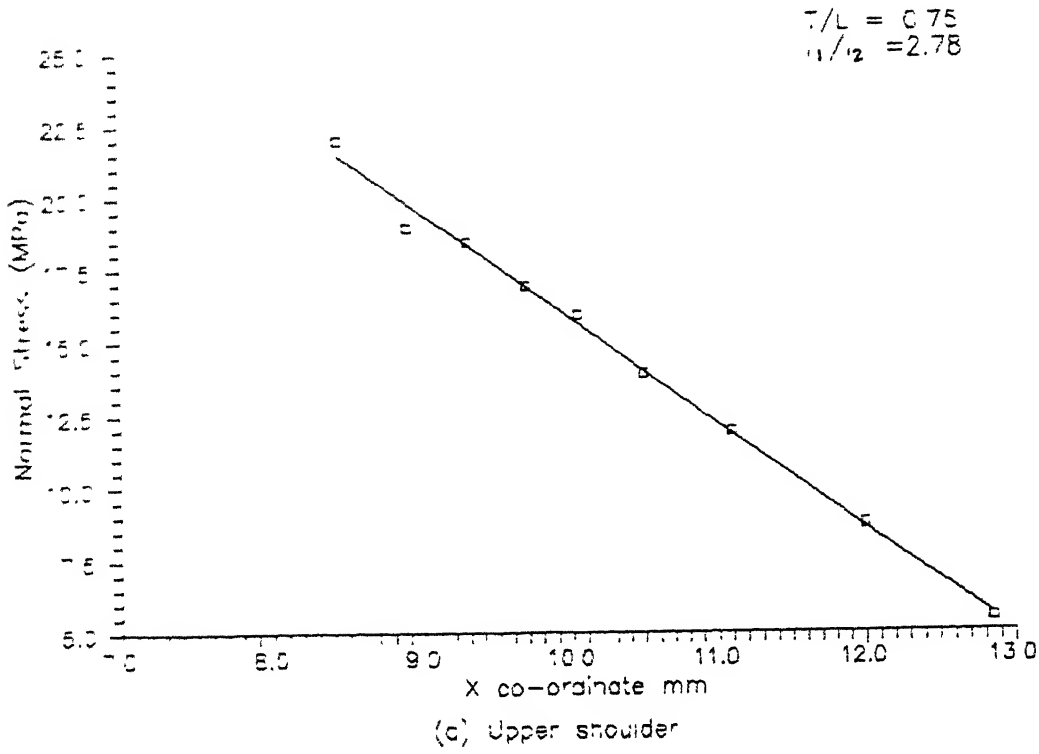

(c) Upper shoulder

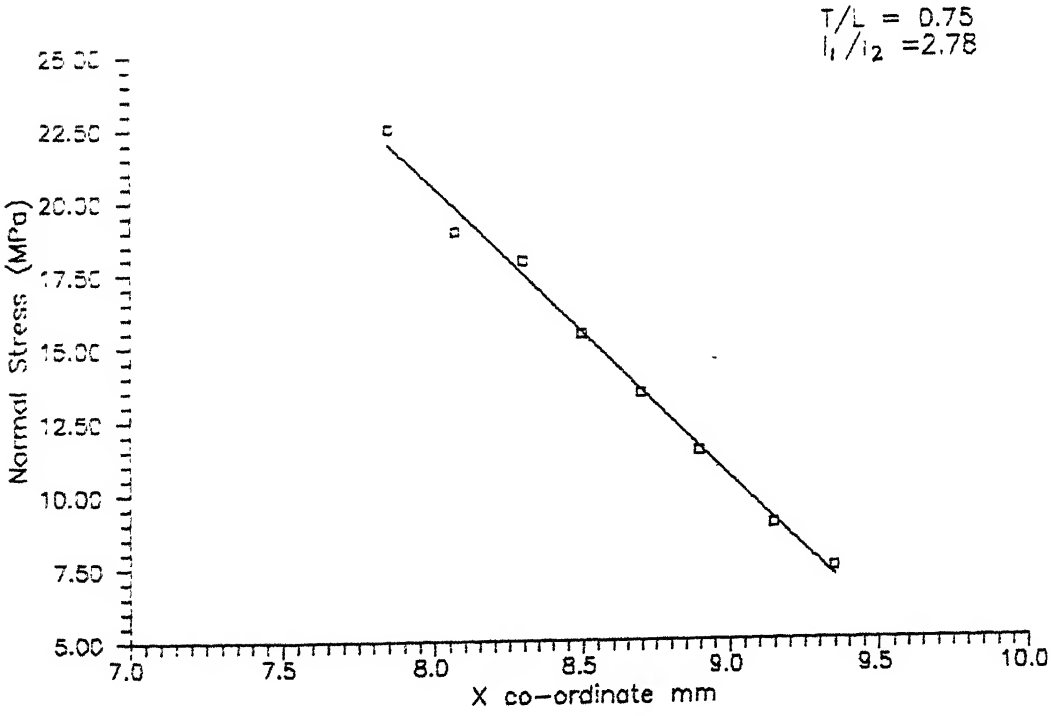

(b) Lower shoulder

Fig.3.20 Variation of normal stress along the contact length (for straddle root, model I)

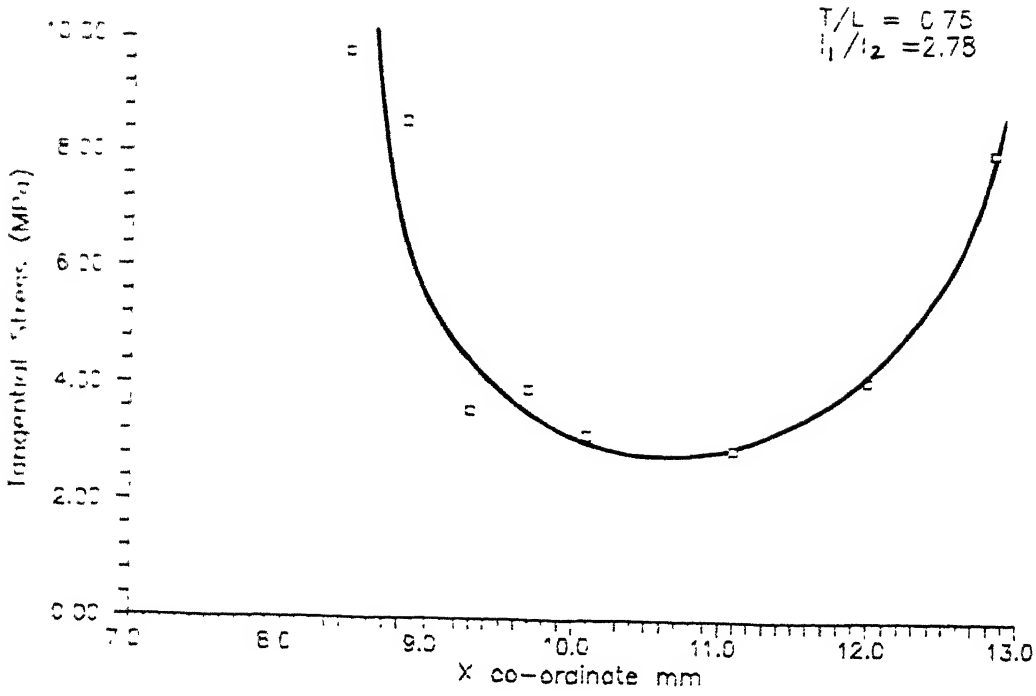

(c) Upper shoulder

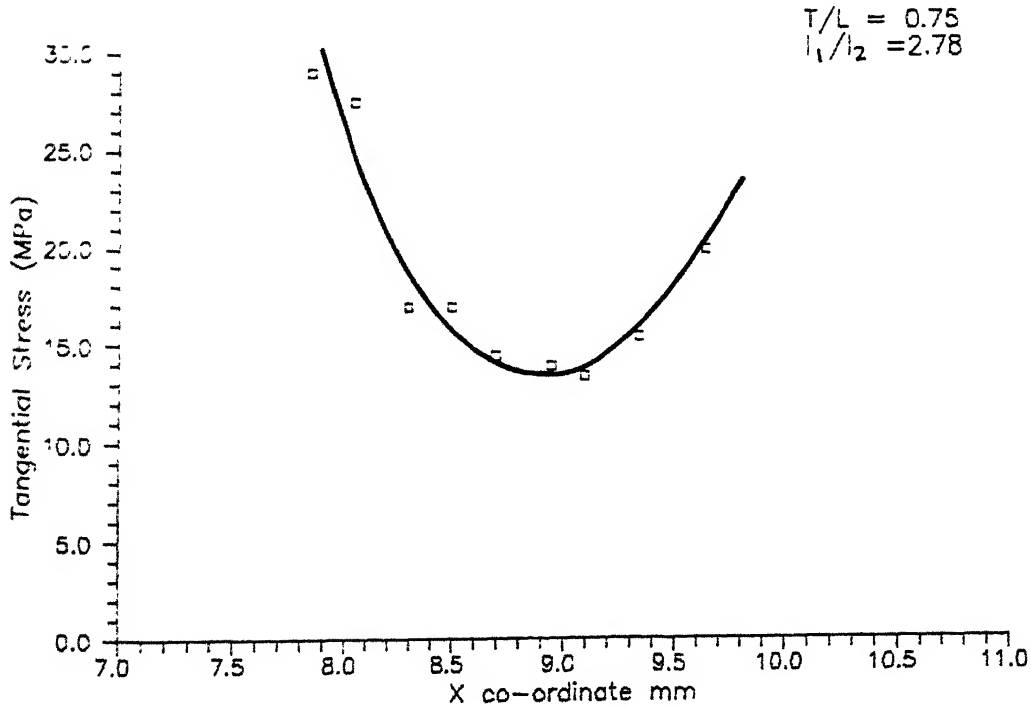

(b) Lower shoulder

Fig.3.21 Variation of tangential stress along the contact length (for straddle root, model 1)

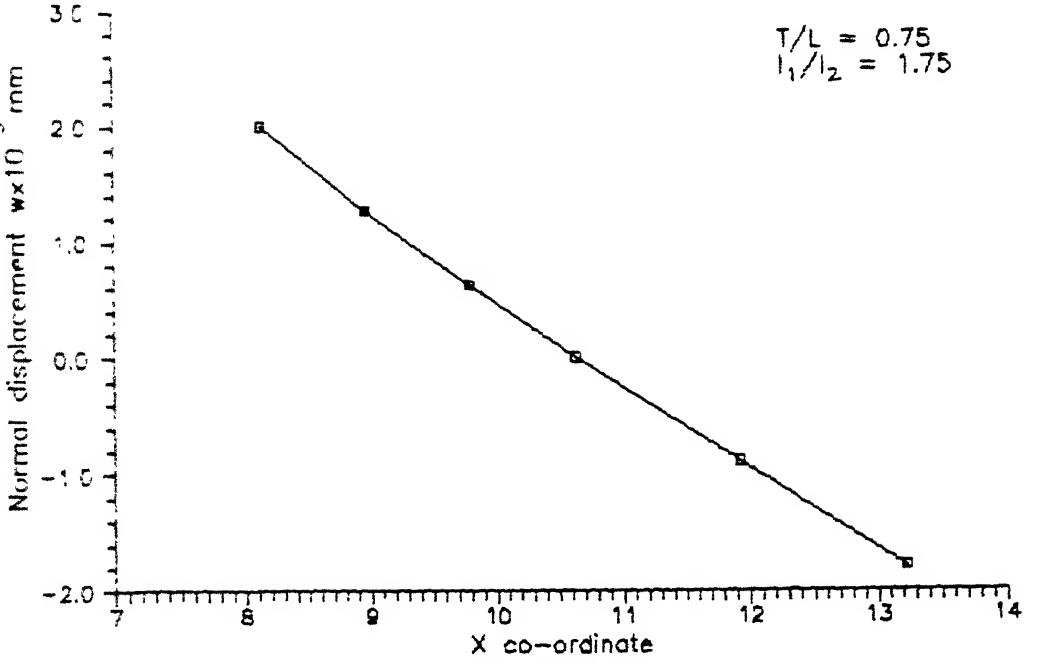

(a) Upper shoulder

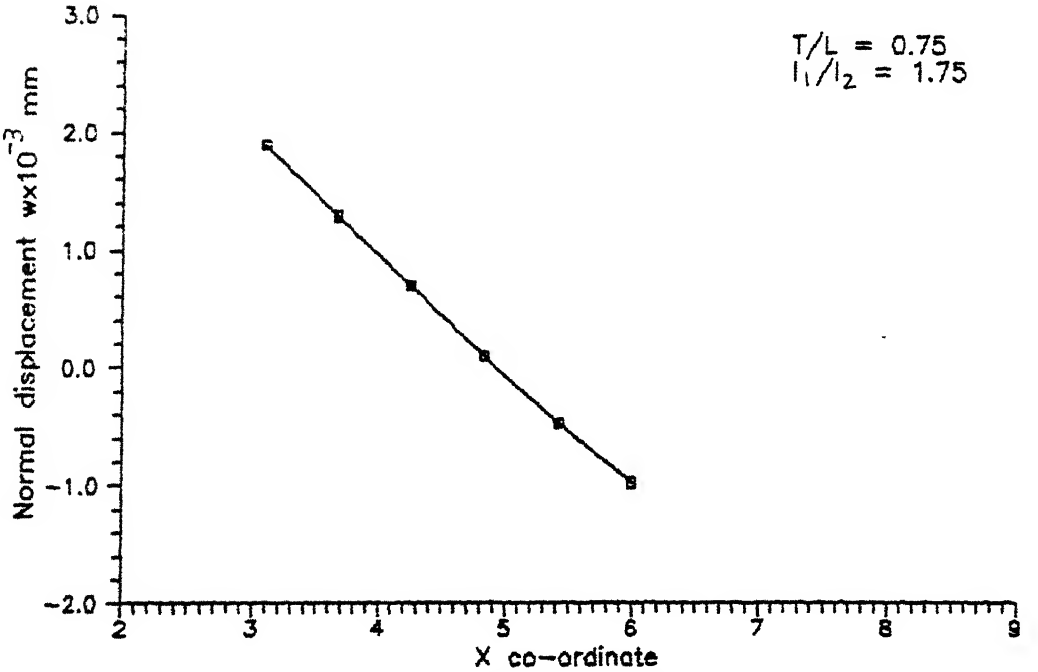

(b) Lower shoulder

Fig.3.22 Variation of normal displacement along the contact length (for straddle root, model II)

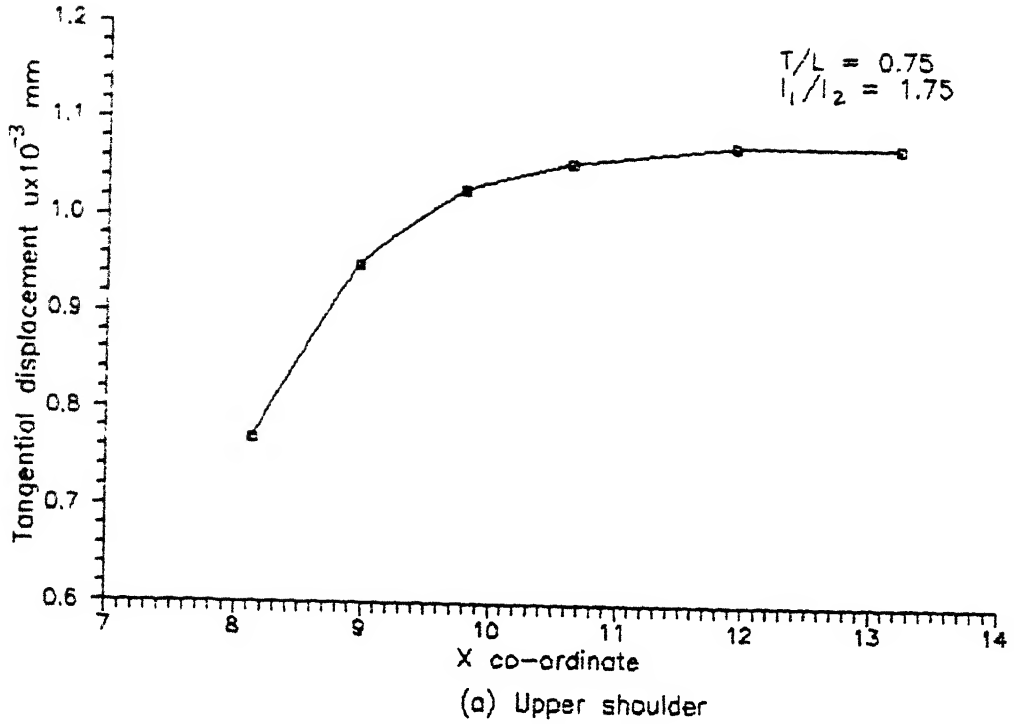

(a) Upper shoulder

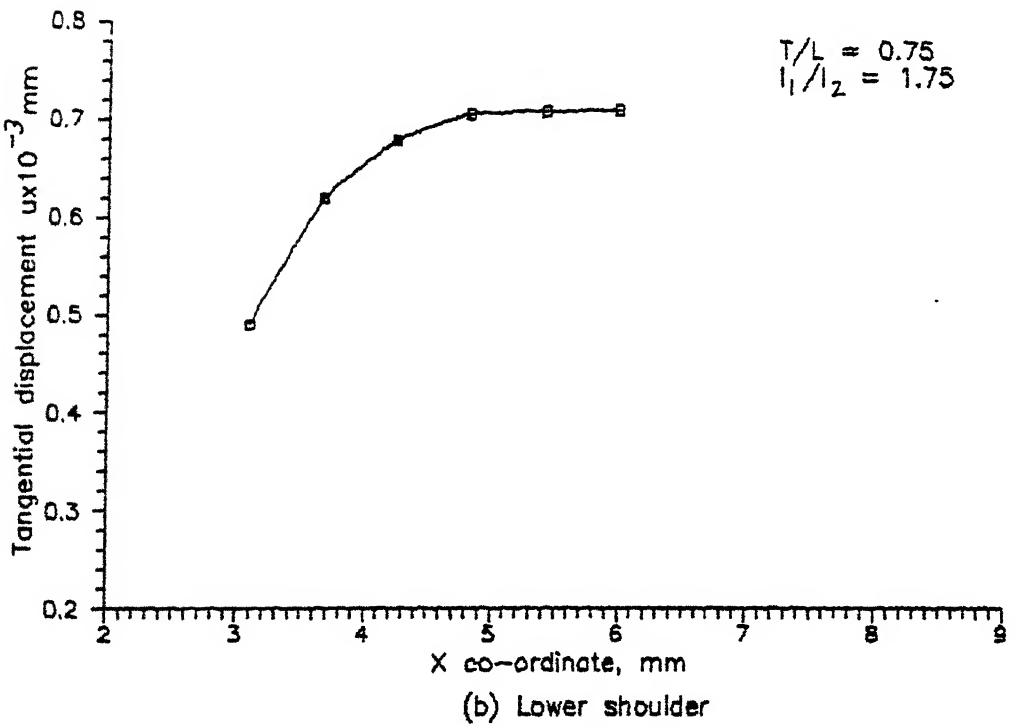

(b) Lower shoulder

Fig.3.23 Variation of tangential displacement along the contact length (for straddle root, model II)

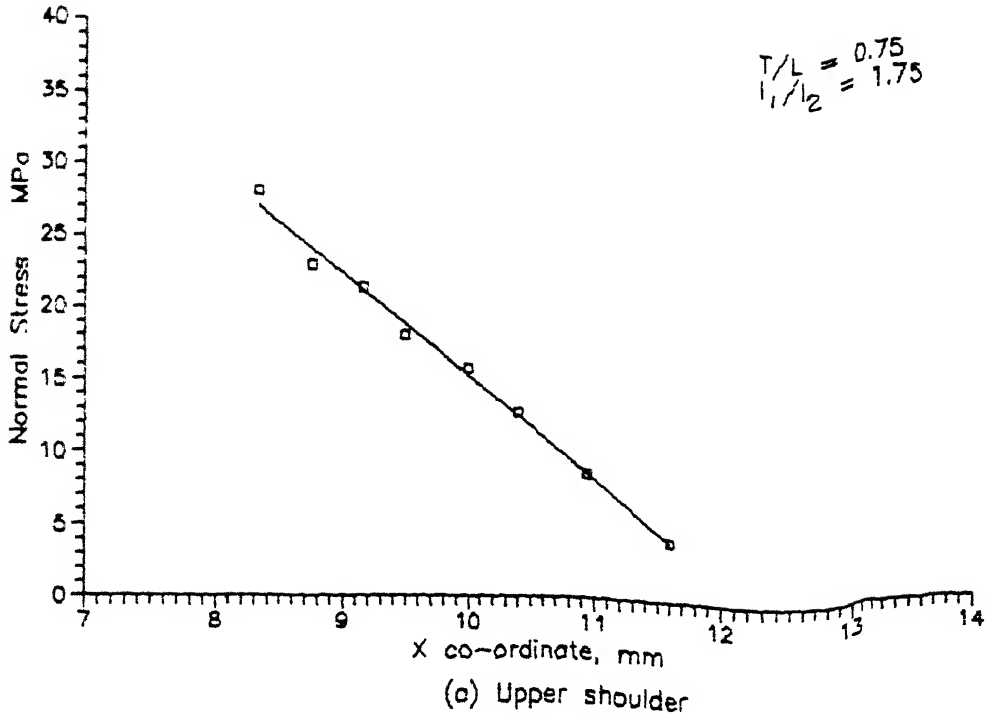

(a) Upper shoulder

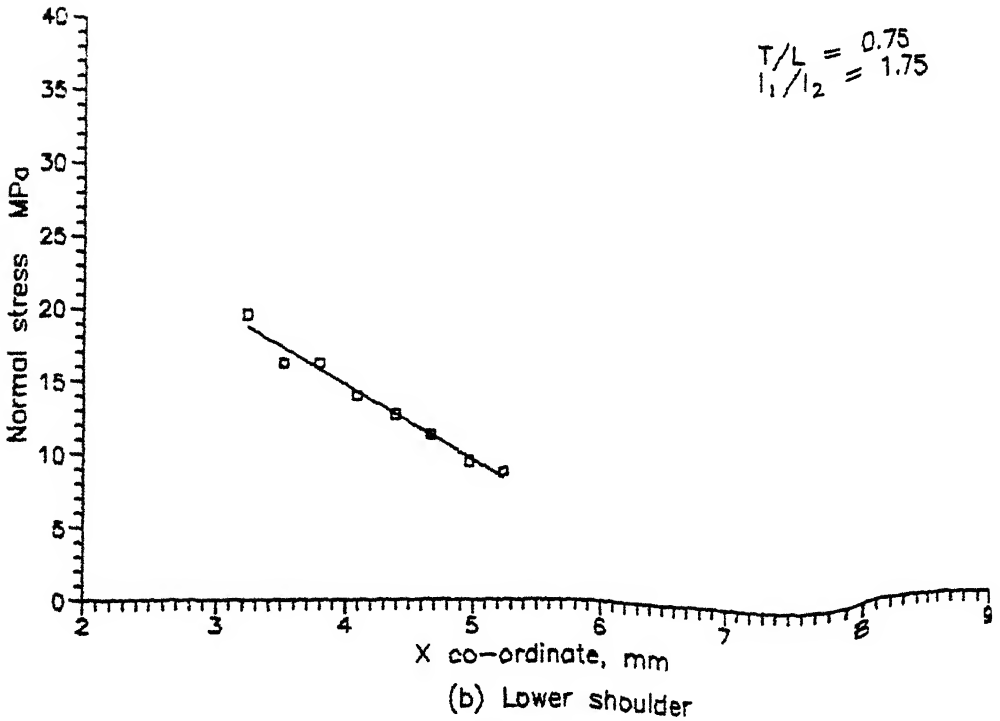

(b) Lower shoulder

Fig.3.24 Variation of normal stresses along the contact length (for straddle root, model II)

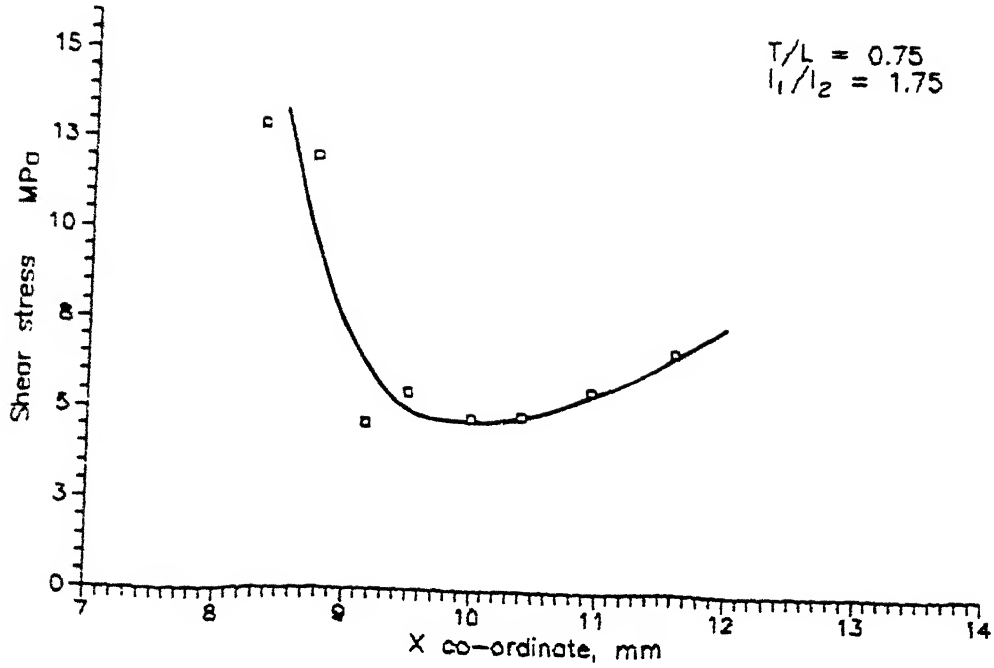

(a) Upper shoulder

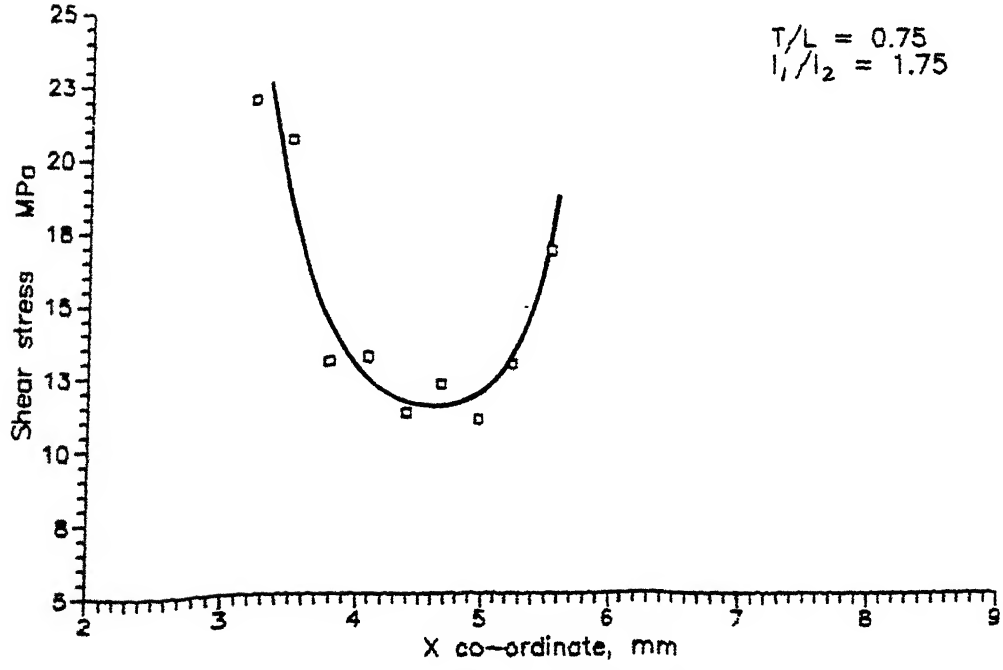

(b) Lower shoulder

Fig.3.25 Variation of shear stresses along the contact length (for straddle root, model II)

indicate parabolic variation. The erratic behaviour of the tangential stress may be due to the application of the slip boundary condition. This boundary condition is applied to the nodal forces rather than to the stress components on the contact surface. If it were possible to apply the slip boundary condition directly to the stresses, then probably the behaviour of the tangential stress would be more smooth.

CHAPTER IV

CONCLUSIONS AND SUGGESTIONS FOR THE FUTURE WORK

The following conclusions can be drawn on the basis of the results presented in Chapter III :

(1) For the given T/L ratio, optimum straddle root is better if T/L ratio is roughly less than 1.5. This, however is only from the strength point of view and that too under steady conditions. When T/L ratio is roughly more than 1.5 tee-root should be used.

(2) Among the models of the optimum straddle roots, the second model is slightly better as it has a lower value of equivalent stress.

(3) Among various straddle roots of the given T/L ratio, the optimum straddle root is the most desirable as it has the same equivalent stress at the corner points.

As mentioned in Chapter I, this work has several limitations in the form of idealisations made. In future, some or all of these can be accounted for, in particular the following modifications can be undertaken :

(1) In case of straddle root, L should be varied to find the optimum ratio of shoulder lengths i.e. $(l_1/l_2)_{opt}$.

(2) The effect of nozzle forces should be considered. The results of this study may change completely with the inclusion of unsteady stresses.

(3) Stagger of blade and radial placing of the root should be considered. Hence the root region should be analysed as a three dimensional contact problem.

REFERENCES

[1] Hertz, H., "On the Contact Problem of Elastic Solids," J. of Math., Vol. 92, pp. 156-171, 1882, (in German), Misc. papers (in English) by Hertz, Jones and Scbott, Macmillon, London, 1896.

[2] Shtaerman, I. Ya., "Generalisation of Hertz Theory of Local Deformations in Elastic Bodies in Compression, "Competes rendus de "academic des science de" U.S.S.R. Vol. XXIX, No. 3, pp. 179-181, 1940.

[3] Muskhelishvili, N.I., "Some Basic Problems of the Mathematical Theory of Elasticity", Nordhoff, The Netherlands, 1963.

[4] Gladwell, G.M.L, "Contact Problems in the Classical Theory of Elast i city", Sijithoff and Nordhoff, The Netherland, 1973.

[5] Francavilla, A. and Zienkiewicz, O.C., "A note on the Numerical Computation of Elastic C o ntact Problems", Int. J. Num. Meth. Engg., Vol-9, pp 913-924, 1975.

[6] Okamota, N. and Nakazawa, M., "Finite Element Incremental Contact Analysis with various Frictional conditions",Vol-14, pp 337-357, 1979.

[7] Hung, N.D. and Sauxe, G., "Frictionless Contact of Elastic Bodies by Finite Element Method and Mathematical Programming Techniques", Computers and Struct., Vol-11, pp 56-67, 1980.

[8] Sachdeva, T.D., Ramakrishnan, C.V. and Natarajan, R., "A Finite Element Method for the Elastic Contact Problems", J. of Appl. Mech., Vol-103, pp 456-461, 1981.

[9] Sachdeva, T.D. and Ramakrishnan,C.V, "A Finite Element Solution for the T wo Dimensional El a stic Contact Problems with Friction", Int. J. Num. Meth. Engg.,Vol-17, pp 1257-1271, 1981.

[10] Torstenfelt, B., "Contact problems with Friction in General Purpose Finite Element Computer Program", Computers and Struct., Vol-16, pp 487-493, 1983.

[11] Rahman, M.V., Rowlands, R.E. and Cook, R.D., "An Iterative Procedure for Finite Element Stress Analysis of Frictional Contact Problems", Vol-14, pp 947-954, 1984.

[12] Bathe, K.J. and Chaudhary, A., "A Solution Method for Plannar and Axisymmetric Contact Problems", Int. J. Num. Meth. Engg., Vol-21, pp 65-88, 1985.

[13] Chandrasekhara, N., Haister, W.E. and Goforth, R.E., "A Finite Element Solution Method for Contact Problems with

Friction", Vol-24, pp 477-495, 1987.

[14] Chan, S.K. and Tuba, I.S., "A Finite Element Method for Contact Problems of Solid Bodies, Part I - Theory and Validation, Part II - Application to turbine blade fastening", Int. J. Mech. Sci., Vol-13, pp 615-639, 1971.

[15] Shrivastava, J.P., " Dynamic Stress Analysis in the Root Region of a Turbine Blade", M. Tech. Thesis, Dept. of Mech. Engg., I.I.T. Kanpur, 1989.

[16] Vyas, N.S., "Vibratory Stress Analysis and Fatigue Life Estimation of Turbine Blade", Ph. D. Thesis, Dept. of Mech. Engg., I.I.T. Delhi, 1986.

[17] Church, E.F., "Steam Turbine", Mc-Graw Hill Book Company Inc., 1950.

[18] Kearton, W.J., "Steam Turbine Theory and Practice", The EnglishLanguage Book Society and Sir Isaac Pitman and Sons Ltd., 1962.

[19] Lee, J.F., "Theory and Design of Steam and Gas Turbine", Mc-wGraw Hill Book Company Inc., 1954.

ME-1990-M-CHA-CHI